Enpp1 inhibits ectopic joint calcification and maintains articular chondrocytes by repressing Hedgehog signaling

Yunyun Jin[1,2], Qian Cong[1], Jelena Gvozdenovic-Jeremic[3], Jiajie Hu[1], Yiqun Zhang[1], Robert Terkeltaub[4], Yingzi Yang[1*]

[1]Harvard School of Dental Medicine, Boston, MA 02115, USA; [2]Shanghai Key Laboratory of Regulatory Biology, institute of Biomedical Sciences and School of Life Sciences, East China Normal University, Shanghai 200241, China; [3]National Human Genome Research Institute, Bethesda, MD 20892, USA; [4]Department of Medicine, Veterans Affairs Healthcare System, University of California San Diego, 111K, 3350 La Jolla Village Dr., San Diego, CA 92161

*Corresponding author:

Yingzi Yang, PhD
Professor of Developmental Biology
Harvard School of Dental Medicine
Harvard Stem Cell Institute
188 Longwood Avenue
Boston, MA 02115
Tel: 617-432-8304
yingzi_yang@hsdm.harvard.edu

Key words: Enpp1, Hedgehog signaling, *Gnas*, Osteoarthritis, Ectopic calcification

Summary statement: Activation of Hedgehog signaling contributes to joint calcification induced by loss of *Enpp1* function

Abstract

The differentiated phenotype of articular chondrocytes of synovial joints needs to be maintained throughout life. Disruption of the articular cartilage, frequently associated with chondrocyte hypertrophy and calcification, is a central feature in osteoarthritis (OA). However, the molecular mechanisms whereby phenotypes of articular chondrocytes are maintained and pathological calcification is inhibited remain poorly understood. Recently, the ecto-enzyme *ENPP1,* a suppressor of pathological calcification, was reported to be decreased in joint cartilage with OA in both human and mouse, and *Enpp1* deficiency causes joint calcification. Here we found that Hedgehog signaling activation contributes to ectopic joint calcification in the *Enpp1*$^{-/-}$ mice. In the *Enpp1*$^{-/-}$ joints, Hedgehog signaling was upregulated. Further activation of Hedgehog signaling by removing *Patched 1* in the *Enpp1*$^{-/-}$ mice enhanced ectopic joint calcification, while removing *Gli2* partially rescued the ectopic calcification phenotype. Additionally, reduction of $G\alpha_s$ in the *Enpp1*$^{-/-}$ mice also enhanced joint calcification, suggesting Enpp1 inhibited Hedgehog signaling and chondrocyte hypertrophy by activating $G\alpha_s$-PKA signaling. Our findings provide new insights in the mechanisms underlying *Enpp1* regulation of joint integrity.

Introduction

The joint connects neighboring skeletal elements together as a functional unit. The joint cartilage protects the underlying bone from excessive mechanical load, which is distributed across the entire joint surface. The healthy synovial joint is composed of articular cartilage and other joint tissues such as synovial membrane and joint ligament (Lories and Luyten, 2011). In the healthy joint, the matrix of articular cartilage maintains a relatively low turnover rates, and chondrocytes exhibit low proliferation rates without hypertrophy or terminal differentiation (Dreier, 2010).

The integrity of the complex joint structures has to be maintained throughout life, disruption of which causes arthritis, a joint disease affecting more than half of the people over the age of 65, and is among the leading causes of disability throughout the world (Guilak, 2011). Osteoarthritis (OA) is the most common type of arthritis (Arai et al., 2004). OA is primarily characterized by cartilage breakdown, which is associated with new bone formation at the joint margins (osteophytosis), subchondral bone sclerosis, variable degrees of mild synovitis, and thickening of the joint capsule (Sellam and Berenbaum, 2010). Articular cartilage loss is the first sign of OA, breakdown of cartilage extracellular matrix leads to an early and high incidence of OA (Heinegard and Saxne, 2011). In the osteoarthritic joint, there is ectopic chondrocyte hypertrophy evidenced by expression of *Collagen 10a1* (*Col 10a*1) and *matrix metalloproteinase 13* (*Mmp13*) (Kamekura et al., 2006; Neuhold et al., 2001) in articular cartilage and these ectopic hypertrophic chondrocytes form calcified cartilage zones (Tchetina, 2011). However, despite detailed histological characterization of OA, the underling molecular mechanisms whereby articular cartilage degeneration is initiated and advanced leading

to OA remain poorly understood. This has severely hampered development of pharmacological agents that can prevent or reduce articular cartilage degeneration and ectopic calcification associated with OA. Multiple risk factors such as hormones, age, and levels of calcium (Ca^{2+}), phosphate (P_i) and pyrophosphate (PP_i) in the blood, have been found to contribute to OA onset and progression. As OA heritability has been suggested to be 50% or more, genetic susceptibility contributes significantly to OA (Spector and MacGregor, 2004; Valdes et al., 2008).

Ectonucleotide pyrophosphatase/phosphodiesterase 1 (Enpp1) is an ecto-enzyme that converts ATP to AMP and PP_i outside of the cells. Enpp1 plays an essential role in phosphate homeostasis (Goding et al., 2003). Enpp1 has been found to be expressed in various cells including chondrocytes and osteoblasts (Goding et al., 1998) and Enpp1 protein has been detected in articular cartilage in both human and mouse joints (Bertrand et al., 2012). Enpp1 inhibits hydroxyapatite formation by generating PP_i, and thereby inhibits soft tissue calcification (Stefan et al., 2005). In human, loss-of-function *ENPP1* mutations cause generalized arterial calcification of infancy (GACI) (Ruf et al., 2005; Rutsch et al., 2003) or Pseudoxanthoma elastic (Nitschke and Rutsch, 2012) and Enpp1 also represents an important genetic susceptibility factor in hand OA, which is the third most common OA, after knee OA and hip OA. A family-based association study showed that genetic variation at the *ENPP1* locus is involved in the etiology of hand OA (Gabay and Gabay, 2013). In mice, loss of function of *Enpp1* results in ectopic calcification of articular cartilage and joint capsule and certain tendons (Babij et al., 2009) (Harmey et al., 2004; Zhang et al., 2016). *Enpp1*$^{-/-}$ mice also exhibit OA-like changes (Bertrand et al., 2012).

Hedgehog (Hh) signaling plays an essential and pivotal role in regulating chondrocyte proliferation and hypertrophy during endochondral bone development, in which *Ihh* is expressed in prehypertrophic and early hypertrophic chondrocytes (Long et al., 2001; Mak et al., 2008b; St-Jacques et al., 1999; Vortkamp et al., 1996). We have shown previously that Hh signaling activation promotes chondrocyte hypertrophy in articular cartilage and Hh signaling activation has been found in human OA (Lin et al., 2009; Mak et al., 2008b). Blockade of Hh signaling can reduce the severity of OA in mice (Lin et al., 2009). We have also found that $G\alpha_s$ inhibits Hh signaling (Regard et al., 2013). In addition, loss of *Gnas*, which encodes $G\alpha_s$, led to premature chondrocyte hypertrophy (Bastepe et al., 2004). As ATP and its derived products such as adenosine generated by Enpp1 can signal through G protein-coupled receptors (GPCR) that can be coupled to $G\alpha_i$ or $G\alpha_s$, Enpp1 may inhibit joint calcification by inhibiting Hh signaling through reducing $G\alpha_i$ signaling and/or upregulating $G\alpha_s$ signaling. To test this hypothesis, here we have determined whether Hh signaling is altered in the *Enpp1*$^{-/-}$ joint. We found ectopic upregulation of Hh signaling activity in the articular cartilage of the *Enpp1*$^{-/-}$ mice. Hh signaling activation by removing one copy of *Ptch1* or reduction by removing one copy of *Gli2* led to enhanced or reduced ectopic joint calcification in the *Enpp1*$^{-/-}$ mice, respectively. In addition, heterozygous loss of *Gnas* function also enhanced the joint calcification phenotypes of the *Enpp1*$^{-/-}$ mice. Our work suggests that apart from regulating ATP, PP_i, and P_i homeostasis, *Enpp1* deficiency may also cause OA by promoting calcification via activating the Hh signaling pathway.

Materials and methods

Animals and diet

The mouse lines have described previously : *Enpp1*$^{-/-}$ mice (*C57BL/6-Enpp1tm1*) (Serrano et al., 2014); *Gnas* $^{f/f}$ (Chen et al., 2005), *Ptch1*$^{+/-}$ (Mak et al., 2008a), *Gli2*$^{+/-}$ (Bai and Joyner, 2001) and *Osterix (Osx)-GFP::Cre* mice (Rodda and McMahon, 2006). Genotyping was done using tail genomic DNA by standard PCR-based procedures. Mice were maintained on normal laboratory diet. Mice of the same genetic background were generated and raised under identical conditions. Female and male mice exhibit similar phenotypes. As the genetic experiments require large number of females in the breeding to obtain appropriate number of mice with desired genotypes, we only used males for experiments. Sex matched litter mate mice were compared. All mouse experiments were approved by the IACUC of NIH and Harvard Medical School.

Histological analysis of the inter-phalangeal joints

Histological analysis was performed on the paraffin sections of the metacarpophalangeal joints of the forelimbs. Skeletal tissues were fixed in 4% paraformaldehyde (wt/vol) overnight at 4 °C, decalcified for one week in 0.5 M EDTA pH 8.0 and dehydrated. Paraffin embedded tissue was sectioned (7 μm) and stained with Safranin O and Hematoxylin & Eosin (H&E) according to standard procedures. Whole-mount X-gal staining was performed as previously described (Topol et al., 2003).

Radiography of skeleton

X-ray images of the fixed forelimbs were taken using Bruker Imager, MS FX PRO.

Immunostaining

Forelimbs were collected and immediately fixed in 4% paraformaldehyde (wt/vol) overnight at 4 °C. Then limbs were decalcified in 0.5M EDTA, pH 7.4 for two weeks at 4 °C, changing EDTA every 3–4 d. The limbs were placed in 30% (wt/vol) sucrose at 4 °C overnight, embedded in OCT and sectioned at 16 μm. The slides were blocked in 5% (wt/vol) BSA in PBST (PBS with 0.02% Tween-20) at room temperature for 1 h, then incubated with primary antibodies diluted in blocking buffer overnight at 4 °C. The slides were washed in PBST 3 × 10 min, incubated in secondary antibodies for 1 h at room temperature, and washed in PBST 3 × 10 min before imaging. Primary antibodies used in immunostaining include anti-Gli1 (Santa Cruz) at 1:50, anti-Col1a1 (Santa Cruz sc-59772) at 1:500, anti-Osx (abcam 22552) at 1:400, anti-Opn (R&D AF808) at 1:500, Anti-Oc (LS-C42094, LifeSpan Biosciences) at 1:100, anti-Sox9 (abcam 185966) at 1:400. To quantify immunostaining, the immunopositive cells were counted in a field of view that have intensity greater than the background by Photoshop CS6. The total area of each field of view were counted by Image J and at least three field of views were counted for each immunostaining.

Isolation, culturing and analyses of SMP, MEF, chondrocytes and synoviocytes.

Subcutaneous skin tissue containing adipose deposits were dissected from 6 weeks old mice. The subcutaneous tissue was prepared under sterile conditions and washed in PBS supplemented with 100U/ml penicillin and 100μg/ml streptomycin on ice. Tissue was minced and digested with 1mg/ml collagenase type1 and 0.5% trypsin in 0.1% BSA at 37°C for 2h, then centrifuged at 650g for 10 min and the floating fat depots were removed, the cell pellets were collected, dissociated and centrifuged a second time at 650g for 10 min. The SMP cell pellet was dissociated and filtered through a 100-μm mesh filter. SMP cells were cultured in Alpha-MEM with 20% FBS, 100U/ml penicillin, 100μg/ml streptomycin, 2mM glutamine. 2.5×10^5 cells were seeded per well in 12-well plates and switched into osteogenic medium with ascorbic acid and glycerophosphate after reaching super confluence. MEF cells were isolated from E12.5-E13.5 mouse embryos. The internal organs of the embryos were removed from the abdominal cavity. Embryos were rinsed in 10 to 20 ml DPBS and transferred to a 15 ml tube containing 3 to 5 ml trypsin/EDTA solution and incubated for 20 min at 37°C. The digested cells were collected and large tissue pieces were avoided. The suspended cells were then centrifuged for 5 min at 1000 × g at room temperature. The cells in the pellets were dissociated in 10 to 50 ml fresh MEF medium with penicillin/streptomycin and plated in 100 mm tissue culture plates or 75-cm^2 flasks. Primary chondrocytes were isolated from P0 mice. The rib cages were incubated with pronase for 30min at 37°C, followed by 3mg/ml collagenase in DMEM at 37°C for 1h 30min until all soft tissues detached from the cartilages with a few pipetting. The cartilage was digested with collagenase for 4-5h and chondrocytes were harvested cells by centrifugation. Synovial cells were isolated

from synovial membranes of the knee joints of 10-week-old mice after digestion with 0.2% collagenase in DMEM at 37 °C for 1 hr. ATP (Sigma FLAAS-1VL), non-hydrolyzable ATP analog (NHATP) (Sigma, A2647) and SAG (MedChem Express, HY-12848) were used in the treatment. Western blotting analysis was performed according to standard protocols (Jin et al., 2012). Antibodies used were as follows: rabbit anti-p-Creb(1:2000; Millipore), rabbit anti-Creb (1:2000; Santa Cruz), mouse anti-GAPDH (1:5000; Sigma), mouse anti-tubulin (1:5000; Sigma).

Quantitative RT-PCR

Quantitative PCR was performed to measure the relative mRNA levels. RNA samples were prepared from the forelimbs without skin using Trizol (Invitrogen) with the RNeasy kit (Qiagen). The phalangeal joints between the metacarpal bone and the proximal phalanx (P1) of digit 3 were used for analysis, unless otherwise indicated in the text. cDNA was generated by the SuperScript2 reverse transcriptase kit (Invitrogen) and digested with Dnase1 (Invitrogen). Primers used for amplification are described previously (Regard et al., 2013). Samples were normalized with GAPDH expression.

Whole-mount skeletal preparation and joint size measurements

Mice were skinned and placed in 100% EtOH overnight, then in 100% Acetone for one day. Whole-mount skeletal preparations were performed as described (McLeod, 1980). Mice were then stained with Alcian Blue/ Alizarin Red solution (50 mL staining solution= 2.5 mL 0.3% alcian blue, 2.5 mL 0.1% alizarin red, 2.5 mL 100% glacial acetic acid, 42.5 mL 70% EtOH) for 2 days at 37°C. The mice were then cleared in 1% KOH for 2

days and transferred to 20% glycerol with 1% KOH until soft tissue was transparent. The cleared mice were stored in 80% glycerol. Four mice of each genotype were used for quantification of the forelimb metacarpophalangeal joints size. Statistics shown in text were averages ± SD. The joint sizes were measured by image J as follows: the length of a straight line indicates the diameter of metacarpophalangeal joint size (D1) on the frontal view of the forelimb and is measured as pixels. The midpoint of the proximal phalange was visually determined and the diameter of the proximal phalanges (D2) was similarly measured. Then the ratio of D1/D2 of each digit was calculated as the relative joint size and used in the statistical analysis.

In situ hybridization

Forelimbs for *in situ* hybridization (ISH) were fixed in 10% (vol/vol) formalin at room temperature for 24-36 h. Paraffin sections of 8μm thickness were used to perform RNA *in situ* hybridization. The ISH were carried out using RNAscope (ACDBio) (Wang et al., 2012) 2.0HD Detection Kit according to the manufacture's instruction. Probe used in the study is mCol1α1 (REF:319371, LOT:15258A). The intensity of ISH signal across the various anatomical locations was compared. Whole mount *in situ* hybridization was performed according to an established protocol (Andre et al., 2015).

Statistical Analysis

Quantification was performed from at least 3 independent experimental groups and presented as mean ± standard deviation (SD). Statistical analysis between groups was performed by 2-tailed Student's *t* test to determine significance when only 2 groups were compared. (*P < 0.05, **P < 0.01, ***P < 0.001) and a probability (P) < 0.05 was considered statistically significant. The signal of immunohistochemistry was calculated as the number of positive cells/field of view.

Results

Loss of *Enpp1* altered cell differentiation in joints

The *Enpp1*$^{-/-}$ mice developed stiffened joints around 4 weeks of age on standard rodent diet with progressively mineralized articular cartilage detected from 9 weeks of age (Bertrand et al., 2012; Li et al., 2013; Zhang et al., 2016). To test if mineralization of the articular cartilage is caused simply by deposition of hydroxyapatite on the articular surfaces or there is loss of articular chondrocyte differentiation and ectopic chondrocyte hypertrophy associated with OA in the joints of the *Enpp1*$^{-/-}$ mice, we first examined gene expression by quantitative real time PCR (qRT-PCR) in the metacarpophalangeal joints of the *Enpp1*$^{-/-}$ and wild type (WT) control mice at 1 month of age when there is no joint mineralization yet (Zhang et al., 2016b) (Fig. 1A). In this study, the phalangeal joints between the metacarpal bone and the proximal phalanx (P1) of digit 3 were used for analysis, unless otherwise indicated in the text. The joint tissue was a mixture of cartilage, tendon and synovium. Normal articular chondrocytes strongly express *Col2*, *Aggrecan* (*Acan*) and *Sox9*, but not *Col10*, a marker for hypertrophic chondrocytes. In the joints of the *Enpp1*$^{-/-}$ mice, we found that while *Col2*, *Acan* and *Sox9* expression was

reduced, *Col10* expression was significantly upregulated. To further examine whether there were hypertrophic chondrocyte differentiation in the articular cartilage of the *Enpp1*$^{-/-}$ mice, we examined the presence of hypertrophic chondrocytes cells using the *Osterix* (*Osx*) promoter-driven GFP-fused cre recombinase (*OsxGFPcre*) mouse line (Rodda and McMahon, 2006). *Osx* is expressed in hypertropic chondrocytes and an early marker of committed osteoblast cells (Nakashima et al., 2002). To detect if *Osx* was ectopically expressed in the phalangeal joint, we generated the *OsxGFPcre; Enpp1*$^{-/-}$ mice. The GFP^{+} cells should be either hypertrophic chondrocytes or osteoblasts, which express *Osx*. While the control WT *OsxGFPcre* mice had almost no GFP^{+} cells in the joint, the number of GFP^{+} cells were drastically increased in the articular cartilage and the joint capsule of the metacarpophalangeal joint of the 4 month old *Enpp1*$^{-/-}$ mice (Supplementary Fig. 1A-1A"), whose joint mineralization started around 8-9 weeks of age (Hajjawi et al., 2014; Zhang et al., 2016). In addition, we performed immunofluorescent staining of Osx and Sox9 in the sections of the 1 month old WT and *Enpp1*$^{-/-}$ metacarpophalangeal joints. Osx expression was detected in the articular cartilage of the metacarpophalangeal joints of the *Enpp1*$^{-/-}$ mice, but not in that of the WT ones (Fig. 1B-C'). Conversely, Sox9 expression was reduced the *Enpp1*$^{-/-}$ mice compared to the WT control (Fig. 1D-E'). These results indicate that besides deposition of hydroxyapatite crystals, the *Enpp1*$^{-/-}$ mice formed ectopic hypertrophic chondrocytes and/or osteoblasts in the articular cartilage and joint capsule.

To further confirm that there were ectopic chondrocyte/osteoblast differentiation in the joints of the *Enpp1*$^{-/-}$ mice, we examined expression of other hypertrophic and osteoblast cell markers. We performed *in situ* hybridization using postnatal day 2 (P2) *Enpp1*$^{-/-}$ forelimb joints and found ectopic expression of *Collagen1a1* (*Col1a1*) in the articular cartilage of the *Enpp1*$^{-/-}$ mice and increased *Col1a1* expression in the joint capsule (Fig. 1F, F'). Furthermore, by immunofluorescent staining, we found that expression of Mmp13 and Osteopontin (Opn) were both up-regulated in the articular cartilage in the metacarpophalangeal joints of the 1month old *Enpp1*$^{-/-}$ mice (Fig. 1G-H'"). Taken together, these results indicate that in the phalangeal joints of the *Enpp1*$^{-/-}$ mice, there is ectopic chondrocyte hypertrophy and osteoblastic differentiation before ectopic mineralization could be detected.

Loss of *Enpp1* led to upregulation of Hh signaling in development

Previous studies have demonstrated that Hh signaling promotes chondrocyte hypertrophy and osteoblast differentiation (Lin et al., 2009; Mak et al., 2006; Regard et al., 2013). We hypothesized that Enpp1 may inhibit chondrocyte hypertrophy/osteoblast differentiation in the joint by inhibiting Hh signaling. Loss of *Enpp1* may have resulted in activated Hh signaling, causing ectopic calcification. To test this hypothesis, we first examined expression of Hh target genes: *Gli1*(Bai et al., 2002), *Hhip*(Chuang and McMahon, 1999) and *Ptch1*(Goodrich et al., 1996) in the E15.5 forelimbs by whole mount *in situ* hybridization (WISH). *Gli1, Hhip* and *Ptch1* expression were all upregulated in the forelimbs of the E15.5 *Enpp1*$^{-/-}$ embryos than those of the *WT* controls (Fig. 2A-D, Supplementary Fig.1B, B'). However, we did not detect obvious ectopic expression of Hh target genes outside of their normal expression domains in the

Enpp1$^{-/-}$ embryos. Upregulation of Hh target gene expression in the forelimbs was further confirmed by qRT-PCR analysis of the E15.5 *Enpp1*$^{-/-}$ and WT embryos (Fig. 2E). These results show that early in skeletal formation during embryonic development, Hh signaling was already upregulated in the *Enpp1*$^{-/-}$ limbs.

Since ectopic mineralization in the *Enpp1*$^{-/-}$ mice occurs at 9 weeks after birth (Zhang et al., 2016b), we asked whether ectopic Hh signaling activation in the joint of the *Enpp1*$^{-/-}$ mutants could be detected before ectopic mineralization. We dissected the limbs from the P2 *Enpp1*$^{-/-}$ and WT mice and gene expression was examined by qRT-PCR. Hh target gene (*Gli1, Hhip*, and *Ptch1*) expression was increased in the *Enpp1*$^{-/-}$ mutant (Fig. 3A). Chondrocyte hypertrophy/osteogenic differentiation was also increased in the *Enpp1*$^{-/-}$ mutant as shown by increased expression of osteoblast differentiation markers such as *Osx*, *Col1a1*, and *osteocalcin* (*Oc*)(Fig. 3A). We then further examined Hh signaling activity *in situ* in the joint. A *LacZ* "knock in" null allele of *Ptch1* (Mak et al., 2008b) was used to examine *Ptch1* expression. X-gal staining of the *Ptch1*$^{+/-}$ metacarpophalangeal joints at P2 showed *Ptch1-LacZ* expression in the growth plate and perichondrium region as expected (Fig. 3B, C, Supplementary Fig. 2E). *Ptch1-LacZ* expression in the articular cartilage was much weaker. Interestingly, clustered strong ectopic *Ptch1-LacZ* expression was detected in the articular cartilage and perichondrum (Fig. 3B'-C", Supplementary Fig. 2F-F') in the P2 *Ptch1*$^{+/-}$*; Enpp1*$^{-/-}$ mouse pups. These results indicate that Hh signaling is indeed ectopically activated early after birth in the joint cartilage of the *Enpp1*$^{-/-}$ mice.

As joint mineralization was observed later than Hh signaling upregulation in the *Enpp1*$^{-/-}$ mice, we hypothesized that upregulation of Hh signaling activity may be progressively more severe, which eventually leads to ectopic joint mineralization. To test this, we performed qRT-PCR analysis with forelimb tissues from 1month old *WT*, *Enpp1*$^{+/-}$ and *Enpp1*$^{-/-}$ mice (Fig. 3D). More pronounced increased in the expression of Hh signaling target genes and osteoblast markers were observed in the limb of the *Enpp1*$^{-/-}$ mice compared with that in the *WT* control. The WT control and *Enpp1*$^{+/-}$ mice, which never developed a stiff joint phenotype, had similar expression levels of the Hh target genes. To examine ectopic activation of Hh signaling *in situ* in older mice, we examined *Ptch1-LacZ* expression again in the metacarpophalangeal joint of 3 weeks old mice, prior to ectopic mineralization was detected. We found that *Ptch1-LacZ* expression was increased in the perichondrium and periosteum of the *Enpp1*$^{-/-}$ mutant digit close to the growth plate (compare Fig. 3F with 3E). In the articular cartilage, more cells, particularly those lining the joint surface, showed stronger LacZ staining in the *Enpp1*$^{-/-}$*; Ptch1*$^{+/-}$ mice (Fig. 3F') compared with the *Ptch1*$^{+/-}$ control (Fig. 3E'). It has been reported that the articular cartilage and tendon of the joints were mineralized in the *Enpp1*$^{-/-}$ mutants mice at 3 months of age (Hajjawi et al., 2014; Harmey et al., 2004; Okawa et al., 1998; Zhang et al., 2016). To examine Hh signaling activities at this stage, qRT-PCR analysis was performed using the *Enpp1*$^{-/-}$ forelimb tissue. The results confirmed our finding that Hh target genes were highly expressed in the *Enpp1*$^{-/-}$ joints compared with the controls (Supplementary Fig. 1C). Our results indicate that in the *Enpp1*$^{-/-}$ joints, Hh activity is increased and detected ectopically before ectopic mineralization occurs in the postnatal phalangeal joint.

Since ectopic calcification and *Ptch1-LacZ* expression were found in the digit joint of the *Enpp1*$^{-/-}$ mice, we further examined Gli1 protein expression in the *Enpp1*$^{-/-}$ and *WT* joint at the age of 2 months and 4 months by immunofluorescent staining. Gli1 expression is also a readout of Hh signaling activity (Ingham and McMahon, 2001) and we found it was indeed ectopically detected in the nucleus of chondrocytes in the articular cartilage of digit joints of both 2 months (Fig. 3G-H”’) and 4 months old *Enpp1*$^{-/-}$ mice (Supplementary Fig. 2A-D”). Taken together, these results suggest that in the phalangeal joints of the *Enpp1*$^{-/-}$ mice, Hh signaling was upregulated and this change was associated with ectopic osteoblast differentiation in the phalangeal joints.

Activation of Hh signaling enhanced joint calcification in the *Enpp1*$^{-/-}$ mice

Our observation that loss of *Enpp1* leads to Hh signaling activation in the phalangeal joint suggests that Hh signaling may be a functional target of *Enpp1* in regulating joint integrity. To test this hypothesis genetically, we first set out to determine if there were genetic interactions between *Ptch1* and *Enpp1* in causing OA. As *Ptch1* encodes an inhibitory receptor of Hh signaling pathway (Stone et al., 1996), removing one allele of *Ptch1* provides a sensitized genetic background to better reveal effects of Hh signaling activation. We reasoned that the digit joint calcification phenotype of the *Enpp1*$^{-/-}$ mice should be enhanced by loss of one copy of *Ptch1*, if activation of Hh signaling is causative for this phenotype. Therefore, the *Ptch1*$^{+/-}$*; Enpp1*$^{-/-}$ mice were generated and *Col1a1* expression was examined by in situ hybridization (Fig. 4A-C’, Supplementary Fig. 3A-C). *Col1a1* expression was further increased in the articular cartilage on both sides of the metacarpophalangeal joint of the P2 *Ptch1*$^{+/-}$*; Enpp1*$^{-/-}$ mice compared to the *Enpp1*$^{-/-}$ mice. Osx, Opn and Oc ectopic expression were determined by

immunohistochemistry and found to be further increased in the *Ptch1*$^{+/-}$; *Enpp1*$^{-/-}$ joints compared to the *Enpp1*$^{-/-}$ joints (Fig. 4D-F'", Supplementary Fig3 D-D"'). These results indicate that phenotypes of ectopic chondrocyte hypertrophy and/or osteoblast differentiation in the *Enpp1*$^{-/-}$ mutant joint were further enhanced by genetic enhancement of Hh signaling.

Consist with increased expression of osteoblast markers in the metacarpophalangeal joint of the *Ptch1*$^{+/-}$; *Enpp1*$^{-/-}$ neonatal mice, in the 3 months old *Ptch1*$^{+/-}$; *Enpp1*$^{-/-}$ mice, joint calcification indicated by Alizarin red staining was enhanced compared with the *Enpp1*$^{-/-}$ mice (Fig. 4G-J). The joint size was quantified by measuring the relative size of the metacarpophalangeal joints using image J (Supplementary Fig. 3E). The relative sizes of metacarpophalangeal joints of digit 2 and 4 were further increased in the *Ptch1*$^{+/-}$; *Enpp1*$^{-/-}$ mice compared to those in the *Enpp1*$^{-/-}$ mice (Fig. 4G-J, N=4). There was no significant difference in the relative size of *WT* and *Enpp1*$^{+/-}$ joints and both were smaller than the *Enpp1*$^{-/-}$ and *Ptch1*$^{+/-}$; *Enpp1*$^{-/-}$ joints. In addition, we compared mineralization levels of the hindlimbs from 4 months old mice by X-ray imaging, which also showed that loss of one copy of *Ptch1* enhanced calcification in the joint area of the *Enpp1*$^{-/-}$ mice (compare Fig. 4N with 4L). These results indicate that activation of Hh signaling in the *Enpp1*$^{-/-}$ mice further promoted osteoblast differentiation in the joint. We then examined cartilage matrix integrity by Safranin-O staining of the articular cartilage sections (Kim et al., 2014)(Fig. 4O-Q'). More severe loss of Safranin-O staining was observed in the metacarpophalangeal joint sections from the *Ptch1*$^{+/-}$; *Enpp1*$^{-/-}$ mice than the *Enpp1*$^{-/-}$ mice at the age of 3 months

(Fig. 4O-4P'). These results indicate that increased Hh signaling further enhanced articular cartilage damage and joint calcification caused by *Enpp1* loss.

Reduced Hh signaling activity partially rescued joint calcification in the *Enpp1*$^{-/-}$ mice

Since Hh signaling promotes chondrocyte hypertrophy as well as osteoblast differentiation (Lin et al., 2009; Mak et al., 2008b; Regard et al., 2013), we next asked whether joint calcification in the *Enpp1*$^{-/-}$ mice can be reduced by inhibiting Hh signaling activity. Gli2 is mainly responsible for the activated form of Gli transcription factors that activate Hh signaling target gene expression (Ahn and Joyner, 2004; Bai et al., 2002; Bai et al., 2004; Corrales et al., 2004; Joeng and Long, 2009). To reduce Hh activity in the *Enpp1*$^{-/-}$ mice, we removed one copy of *Gli2* (Fig. 5D, D', H), and found this led to decreased joint sizes compared to those in the *Enpp1*$^{-/-}$ mice (N=4 in each group) (Fig. 5A-D', 5I, Supplementary Fig. 4A-C). *Enpp1*$^{+/-}$*; Gli2*$^{+/-}$ mice or *Enpp1*$^{+/-}$ mice didn't show joint calcification and they were considered as control groups (Fig. 5A-5B'). As Hh signaling promotes osteoblast differentiation from mesenchymal progenitor cells, we next tested whether *Enpp1* inhibits osteoblast differentiation from mesenchymal progenitor cells by inhibiting Hh signaling. Subcutaneous mesenchymal progenitors (SMPs) were isolated from the *Enpp1*$^{-/-}$*; Gli2*$^{+/-}$, *Enpp1*$^{-/-}$, *Enpp1*$^{+/-}$*; Gli2*$^{+/-}$ and *Enpp1*$^{+/-}$ mice and cultured under osteogenic conditions. Osteoblast differentiation was determined by alkaline phosphatase (ALP) staining and qRT-PCR assays. ALP activities were similar in the control *Enpp1*$^{+/-}$*; Gli2*$^{+/-}$ or *Enpp1*$^{+/-}$ SMPs, but increased in the *Enpp1*$^{-/-}$ SMPs and such increased was ameliorated in the *Enpp1*$^{-/-}$*; Gli2*$^{+/-}$ cells (Fig. 5E-H). Consistently, expression of Hh target genes and osteogenic markers were all

decreased in the *Enpp1*$^{-/-}$*; Gli2*$^{+/-}$ SMPs compared to the *Enpp1*$^{-/-}$ SMPs (Fig. 5J). Therefore, reduction of Hh signaling indeed led to reduce osteoblast differentiation from mesenchyme progenitor cells promoted by loss of *Enpp1*.

Loss of *Gnas* enhanced joint calcification in the *Enpp1*$^{-/-}$ mice

As Hh signaling activation due to *Enpp1* loss contributed to joint calcification in the *Enpp1*$^{-/-}$ mice, we next asked how Enpp1 inhibited Hh signaling. Hh signaling pathway can be inhibited by $G\alpha_s$ signaling (He et al., 2014; Regard et al., 2013) and ATP can signal through $G\alpha_i$ or $G\alpha_s$ coupled receptors (Burnstock, 2007; Di Virgilio, 2012). We therefore tested whether ectopic joint calcification in the *Enpp1*$^{-/-}$ mice can be enhanced by loss of *Gnas* function. The *Enpp1*$^{-/-}$*; Gnas*$^{+/-}$ mice were generated and ectopic calcification of the metacarpal bones and interphalangeal joints were examined at 2 months of age (Fig. 6A-D) (N=3 in each group). Ectopic calcification was not detected in the *Gnas*$^{+/-}$ mice (Fig.6C), but loss of one copy of *Gnas* enhanced joint calcification of the *Enpp1*$^{-/-}$ mice (Compare Fig.6D with Fig.6B). This was also confirmed by Alizarin red and Alcian blue staining of the skeleton of 2.5 months old mice (Fig. 6E, F). The *Enpp1*$^{-/-}$*; Gnas*$^{+/-}$ mice showed most severe calcification and enlargement of the interphalangeal joints, with the reduced space in the phalangeal joint cavity.

We then performed Safranin-O staining of the phalangeal joint sections to detect the cartilage matrix integrity. Articular cartilage was thinner at the age of one month in the *Enpp1*$^{-/-}$*; Gnas*$^{+/-}$ joints compared to the joint from the *Enpp1*$^{-/-}$ mice (Fig.6G-I). Thinner articular cartilage layer in the joint was also found in the *Ptch1*$^{c/c}$*; Col2a1-CreER* mice (Mak et al., 2008b), consistent with the notion that upregulated Hh signaling contributes

to the joint phenotypes. To test whether reduction of *Gnas* is associated with Hh signaling upregulation, we examined expression of Hh signaling target Gli1, chondrocyte hypertrophy/osteoblast differentiation marker Osx and an articular chondrocyte marker Sox9 by immunohistochemistry. We found that while Gli1, Osx were expressed at higher levels in the articular cartilage of the *Enpp1*$^{-/-}$; *Gnas*$^{+/-}$ mice than the *Enpp1*$^{-/-}$ mice, Sox9 expression was reduced (Fig. 6J-R'"). These results indicate that *Gnas* genetically interacts with *Enpp1* to inhibit joint calcification and support that Enpp1 may act through Gα_i to inhibit Hh signaling in the joint cartilage.

The P2 receptors (i.e., P2X and P2Y receptors) mediate ATP signaling (Erb et al., 2006; Khakh and North, 2006). Eight P2Y family members are G protein-coupled receptors (GPCRs) (P2Y1, P2Y2, P2Y4, P2Y6, P2Y11–14), and respond to the extracellular ATP and ADP (North, 2002). In addition, adenosine receptors, which are also GPCRs, respond to adenosine derived from ATP and ADP after hydrolysis. To test whether ectopic calcification in the *Enpp1*$^{-/-}$ mice may be caused by increased extracellular ATP, which can act through Gα_i coupled P2 receptors to inhibit cAMP production and PKA activity, we treated mouse embryonic fibroblast cells (MEF cells) with ATP and detected p-Creb levels as an indication of protein kinase A (PKA) activities, which are positively or negatively regulated by Gα_s or Gα_i through cAMP respectively. MEF cells were treated with 1mM or 1μM of ATP for 5 min. The p-Creb levels were significantly decreased in both ATP treatment cells especially in the 1mM ATP treated one (Fig.6S). To test whether joint cells were similarly regulated, ATP treatment of primary synovial cells was performed, which also resulted in reduction of Creb phosphorylation (Supplementary Fig. 4D). These results suggest that increased

extracellular ATP can decrease cAMP and PKA levels leading to reduction of p-Creb levels. To further test whether chondrocytes were regulated by Enpp1 through ATP, primary chondrocytes were isolated from the WT or *Enpp1*$^{-/-}$ mice and treated with vehicle or 1mM ATP for 5 min, ATP treatment of WT chondrocytes also reduced Creb phosphorylation and *Enpp1*$^{-/-}$ chondrocytes with vehicle treatment showed much lower p-Creb/ total Creb ratio compared with those from the *WT* chondrocytes (Fig. 6T), indicating that loss of Enpp1 in chondrocytes reduced PKA activities due to increased extracellular ATP levels. Furthermore, *Enpp1*$^{-/-}$ chondrocytes lost response to ATP treatment (Fig. 6T), possibly due to saturated ATP levels. These results suggest that in chondrocytes and possibly other synovial tissues, Enpp1 regulates PKA activities, which in turn regulates Hh signaling as has been previously reported in other contexts (He et al., 2014; Regard et al., 2011; Regard et al., 2013).

ATP can be hydrolyzed by Enpp1 to form PP_i and AMP, which can be further hydrolyzed to form Adenosine and Pi. To further test if loss of Enpp1 leads to increased ATP signaling through $G\alpha_i$ to decrease p-Creb, we treated MEF cells with ATP and a non-hydrolyzeable ATP (NHATP, β, γ-CH_2-ATP), which functions as a selective inhibitor of human ENPP1 (Lecka et al., 2013). In the MEF cells, we found that, both ATP and NHATP can efficiently reduce the phosphorylation of Creb at the concentration of 0.1mM for 10 min (Fig. 6U). NHATP appears to have slightly stronger activities than ATP, possibly due to its resistant to hydrolysis. Interestingly, treatment with SAG, an agonist of Hh receptor smoothened (a 7 transmembrane protein), also reduced Creb phosphorylation. These results suggest that Enpp1 in the extracellular space may

promote $G\alpha_s$ signaling activity by reducing ATP-induced $G\alpha_i$ signaling, thereby inhibiting joint calcification.

Discussion

Here we show that upregulated Hh signaling activity contributes to the joint calcification phenotypes of the *Enpp1*$^{-/-}$ mice. Increased Hh signaling activity was observed early in embryonic development of the *Enpp1*$^{-/-}$ embryos. Ectopic expression of Hh target genes together with upregulation of chondrocyte hypertrophy/osteogenic markers preceded joint calcification in the joint of the postnatal *Enpp1*$^{-/-}$ mice. Genetic enhancement or reduction of Hh signaling enhanced or reduced the joint calcification phenotypes in the *Enpp1*$^{-/-}$ mice, respectively. Our work suggests that inhibition of Hh signaling may lead to a therapeutic strategy to reduce ectopic calcification caused by loss or reduced ENPP1 functions in humans.

Extracellular PP_i is a critical factor that inhibits calcification. Enpp1 deficiency directly leads to reduced PP_i levels, causing deposition of hydroxyapatite (Murshed et al., 2005) (Harmey et al., 2004). In this current study, we observed activation of Hh signaling and expression of the chondrocyte hypertrophy/osteoblast markers in the *Enpp1*$^{-/-}$ joint, indicating that calcification caused by *Enpp1* deficiency is not only a process of passive deposition of hydroxyapatite on the joint surface, but is also driven by an active process due to ectopic chondrocyte hypertrophy and/or osteoblast differentiation driven by activated Hh signaling. As recent studies show that chondrocytes can transdifferentiate into osteoblasts (Dy et al., 2012; Park et al., 2015; Yang et al., 2014a; Yang et al.,

2014b; Zhou et al., 2014), it will be interesting to further determine whether osteoblast transdifferentiation indeed occurs in the articular cartilage of the *Enpp1*$^{-/-}$ mice. Our evidence suggests that Hh signaling upregulation is a primary outcome of *Enpp1* deficiency, not a secondary effect of decreased PP_i, as both ATP and NHATP, inhibited PKA activity shown by reduced Creb phosphorylation (Fig. 6U). It is likely that calcification induced by decreased PP_i levels and Hh signaling activation in the joint of the *Enpp1*$^{-/-}$ mice are paralleled processes. This is further supported by partial rescue of ectopic calcification in the *Enpp1*$^{-/-}$ mice by removing one copy of *Gli2*. There are several possibilities why *Gli2*$^{+/-}$ only partially rescued the *Enpp1*$^{-/-}$ stiff joint phenotype. First, whole body PP_i levels were decreased in the *Enpp1* deficient mice (Johnson et al., 2003). Removal of *Gli2* cannot change the circulation P_i/PP_i ratio in the *Enpp1*$^{-/-}$*; Gli2*$^{+/-}$ mice as Hh signaling and PP_i act parallel downstream of *Enpp1*. Second, although we removed *Gli2*, *Gli1* and *Gli3* are still there to transduce Hh signaling. Lastly, *Enpp1* may regulate other signaling pathways to inhibit osteoblast differentiation.

Hh signaling plays critical roles in regulating chondrocyte proliferation and hypertrophy during embryonic development and after birth. Ectopic activation of Hh signaling causes OA in long bone synovial joints (Lin et al., 2009; Mak et al., 2008a). Our findings extended these previous studies by showing that Enpp1 is an important regulator of Hh signaling. Joint calcification was detected in the phalangeal joint cartilage and the soft tissue such as the joint capsule in the *Enpp1*$^{-/-}$ mice. Similar observations have been made in a recent study showing that *Enpp1* loss of function leads to ectopic mineralization in cartilage and soft tissues such as tendons and

ligaments (Hajjawi et al., 2014; Harmey et al., 2004; Zhang et al., 2016). Our results suggest that upregulated Hh signaling activity in the absence of *Enpp1* may be a common mechanism underlying ectopic calcification found in distinct tissues. Except joint calcification, loss of *Enpp1* function also results in vascular calcification (Lorenz-Depiereux et al., 2010; Rutsch et al., 2003), a degenerative process associated with increased risk of cardiovascular problems. Human patients who carry the *ENPP1* loss of function mutations develop vascular calcification described as generalized arterial calcification of infancy (GACI) (Nitschke et al., 2012), which is a rare autosomal-recessive disorder with calcification of the internal elastic lamina, fibrotic myointimal proliferation of muscular arteries (Rutsch et al., 2001). It would be interesting to determine whether arterial calcification and joint calcification share similar mechanisms involving activation of Hh signaling and whether inhibition of Hh signaling could reduce vascular calcification.

Acknowledgements

We thank members of the Yang lab for stimulating discussions. The work in the Yang lab was supported by R01DE025866 and R01AR070877 from NIH. Yunyun Jin is also supported by National Natural Science Foundation of China (Grant No.81702112), Shanghai Sailing Program (Grant No.17YF1404900), and the National Key Research and Development Program of China(2016YFC0902102). Robert Terkeltaub is supported by the Department of Veterans Affairs grant (to RT) I01BX001660 and NIH grant (to RT) AG007996.

Competing interests

The authors declare no competing interests.

Author contributions

Y.J., Q.C., R.T, and Y.Y. designed the experiments and analyzed the data. Y.J. and Y.Y. wrote the manuscript, with critical input from R.T. Y.J., Q.C., J.G.-J, J. H. and Y.Z. performed the experiments described in this study.

References

Ahn, S. and Joyner, A. L. (2004). Dynamic changes in the response of cells to positive hedgehog signaling during mouse limb patterning. *Cell* **118**, 505-516.

Andre, P., Song, H., Kim, W., Kispert, A. and Yang, Y. (2015). Wnt5a and Wnt11 regulate mammalian anterior-posterior axis elongation. *Development* **142**, 1516-1527.

Arai, M., Anderson, D., Kurdi, Y., Annis-Freeman, B., Shields, K., Collins-Racie, L. A., Corcoran, C., DiBlasio-Smith, E., Pittman, D. D., Dorner, A. J., et al. (2004). Effect of adenovirus-mediated overexpression of bovine ADAMTS-4 and human ADAMTS-5 in primary bovine articular chondrocyte pellet culture system. *Osteoarthritis and cartilage / OARS, Osteoarthritis Research Society* **12**, 599-613.

Babij, P., Roudier, M., Graves, T., Han, C. Y., Chhoa, M., Li, C. M., Juan, T., Morony, S., Grisanti, M., Li, X., et al. (2009). New variants in the Enpp1 and Ptpn6 genes cause low BMD, crystal-related arthropathy, and vascular calcification. *Journal of bone and mineral research : the official journal of the American Society for Bone and Mineral Research* **24**, 1552-1564.

Bai, C. B., Auerbach, W., Lee, J. S., Stephen, D. and Joyner, A. L. (2002). Gli2, but not Gli1, is required for initial Shh signaling and ectopic activation of the Shh pathway. *Development* **129**, 4753-4761.

Bai, C. B. and Joyner, A. L. (2001). Gli1 can rescue the in vivo function of Gli2. *Development* **128**, 5161-5172.

Bai, C. B., Stephen, D. and Joyner, A. L. (2004). All mouse ventral spinal cord patterning by hedgehog is Gli dependent and involves an activator function of Gli3. *Dev Cell* **6**, 103-115.

Bastepe, M., Weinstein, L. S., Ogata, N., Kawaguchi, H., Juppner, H., Kronenberg, H. M. and Chung, U. I. (2004). Stimulatory G protein directly regulates hypertrophic differentiation of growth plate cartilage in vivo. *Proc Natl Acad Sci U S A* **101**, 14794-14799.

Bertrand, J., Nitschke, Y., Fuerst, M., Hermann, S., Schafers, M., Sherwood, J., Nalesso, G., Ruether, W., Rutsch, F., Dell'Accio, F., et al. (2012). Decreased levels of nucleotide pyrophosphatase phosphodiesterase 1 are associated with cartilage calcification in osteoarthritis and trigger osteoarthritic changes in mice. *Ann Rheum Dis* **71**, 1249-1253.

Burnstock, G. (2007). Purine and pyrimidine receptors. *Cellular and molecular life sciences : CMLS* **64**, 1471-1483.

Chen, M., Gavrilova, O., Zhao, W. Q., Nguyen, A., Lorenzo, J., Shen, L., Nackers, L., Pack, S., Jou, W. and Weinstein, L. S. (2005). Increased glucose tolerance and reduced adiposity in the absence of fasting hypoglycemia in mice with liver-specific Gs alpha deficiency. *J Clin Invest* **115**, 3217-3227.

Chuang, P. T. and McMahon, A. P. (1999). Vertebrate Hedgehog signalling modulated by induction of a Hedgehog-binding protein. *Nature* **397**, 617-621.

Corrales, J. D., Rocco, G. L., Blaess, S., Guo, Q. and Joyner, A. L. (2004). Spatial pattern of sonic hedgehog signaling through Gli genes during cerebellum development. *Development* **131**, 5581-5590.

Di Virgilio, F. (2012). Purines, purinergic receptors, and cancer. *Cancer research* **72**, 5441-5447.

Dreier, R. (2010). Hypertrophic differentiation of chondrocytes in osteoarthritis: the developmental aspect of degenerative joint disorders. *Arthritis research & therapy* **12**, 216.

Dy, P., Wang, W., Bhattaram, P., Wang, Q., Wang, L., Ballock, R. T. and Lefebvre, V. (2012). Sox9 directs hypertrophic maturation and blocks osteoblast differentiation of growth plate chondrocytes. *Developmental cell* **22**, 597-609.

Erb, L., Liao, Z., Seye, C. I. and Weisman, G. A. (2006). P2 receptors: intracellular signaling. *Pflugers Archiv : European journal of physiology* **452**, 552-562.

Gabay, O. and Gabay, C. (2013). Hand osteoarthritis: new insights. *Joint, bone, spine : revue du rhumatisme* **80**, 130-134.

Goding, J. W., Grobben, B. and Slegers, H. (2003). Physiological and pathophysiological functions of the ecto-nucleotide pyrophosphatase/phosphodiesterase family. *Biochimica et biophysica acta* **1638**, 1-19.

Goding, J. W., Terkeltaub, R., Maurice, M., Deterre, P., Sali, A. and Belli, S. I. (1998). Ecto-phosphodiesterase/pyrophosphatase of lymphocytes and non-lymphoid cells: structure and function of the PC-1 family. *Immunol Rev* **161**, 11-26.

Goodrich, L. V., Johnson, R. L., Milenkovic, L., McMahon, J. A. and Scott, M. P. (1996). Conservation of the hedgehog/patched signaling pathway from flies to mice: induction of a mouse patched gene by Hedgehog. *Genes Dev* **10**, 301-312.

Guilak, F. (2011). Biomechanical factors in osteoarthritis. *Best practice & research. Clinical rheumatology* **25**, 815-823.

Hajjawi, M. O., MacRae, V. E., Huesa, C., Boyde, A., Millan, J. L., Arnett, T. R. and Orriss, I. R. (2014). Mineralisation of collagen rich soft tissues and osteocyte lacunae in Enpp1(-/-) mice. *Bone* **69**, 139-147.

Harmey, D., Hessle, L., Narisawa, S., Johnson, K. A., Terkeltaub, R. and Millan, J. L. (2004). Concerted regulation of inorganic pyrophosphate and osteopontin by akp2, enpp1, and ank: an integrated model of the pathogenesis of mineralization disorders. *The American journal of pathology* **164**, 1199-1209.

He, X., Zhang, L., Chen, Y., Remke, M., Shih, D., Lu, F., Wang, H., Deng, Y., Yu, Y., Xia, Y., et al. (2014). The G protein alpha subunit Galphas is a tumor suppressor in Sonic hedgehog-driven medulloblastoma. *Nat Med* **20**, 1035-1042.

Heinegard, D. and Saxne, T. (2011). The role of the cartilage matrix in osteoarthritis. *Nature reviews. Rheumatology* **7**, 50-56.

Ingham, P. W. and McMahon, A. P. (2001). Hedgehog signaling in animal development: paradigms and principles. *Genes & development* **15**, 3059-3087.

Jin, Y., Dong, L., Lu, Y., Wu, W., Hao, Q., Zhou, Z., Jiang, J., Zhao, Y. and Zhang, L. (2012). Dimerization and cytoplasmic localization regulate Hippo kinase signaling activity in organ size control. *The Journal of biological chemistry* **287**, 5784-5796.

Joeng, K. S. and Long, F. (2009). The Gli2 transcriptional activator is a crucial effector for Ihh signaling in osteoblast development and cartilage vascularization. *Development* **136**, 4177-4185.

Johnson, K., Goding, J., Van Etten, D., Sali, A., Hu, S. I., Farley, D., Krug, H., Hessle, L., Millan, J. L. and Terkeltaub, R. (2003). Linked deficiencies in extracellular PP(i) and osteopontin mediate pathologic calcification associated with defective PC-1 and ANK expression. *Journal of bone and mineral research : the official journal of the American Society for Bone and Mineral Research* **18**, 994-1004.

Kamekura, S., Kawasaki, Y., Hoshi, K., Shimoaka, T., Chikuda, H., Maruyama, Z., Komori, T., Sato, S., Takeda, S., Karsenty, G., et al. (2006). Contribution of runt-related transcription factor 2 to the pathogenesis of osteoarthritis in mice after induction of knee joint instability. *Arthritis and rheumatism* **54**, 2462-2470.

Khakh, B. S. and North, R. A. (2006). P2X receptors as cell-surface ATP sensors in health and disease. *Nature* **442**, 527-532.

Kim, J. H., Jeon, J., Shin, M., Won, Y., Lee, M., Kwak, J. S., Lee, G., Rhee, J., Ryu, J. H., Chun, C. H., et al. (2014). Regulation of the catabolic cascade in osteoarthritis by the zinc-ZIP8-MTF1 axis. *Cell* **156**, 730-743.

Lecka, J., Ben-David, G., Simhaev, L., Eliahu, S., Oscar, J., Jr., Luyindula, P., Pelletier, J., Fischer, B., Senderowitz, H. and Sevigny, J. (2013). Nonhydrolyzable ATP analogues as selective inhibitors of human NPP1: a combined computational/experimental study. *Journal of medicinal chemistry* **56**, 8308-8320.

Li, Q., Guo, H., Chou, D. W., Berndt, A., Sundberg, J. P. and Uitto, J. (2013). Mutant Enpp1asj mice as a model for generalized arterial calcification of infancy. *Disease models & mechanisms* **6**, 1227-1235.

Lin, A. C., Seeto, B. L., Bartoszko, J. M., Khoury, M. A., Whetstone, H., Ho, L., Hsu, C., Ali, S. A. and Alman, B. A. (2009). Modulating hedgehog signaling can attenuate the severity of osteoarthritis. *Nature medicine* **15**, 1421-1425.

Long, F., Zhang, X. M., Karp, S., Yang, Y. and McMahon, A. P. (2001). Genetic manipulation of hedgehog signaling in the endochondral skeleton reveals a direct role in the regulation of chondrocyte proliferation. *Development* **128**, 5099-5108.

Lorenz-Depiereux, B., Schnabel, D., Tiosano, D., Hausler, G. and Strom, T. M. (2010). Loss-of-function ENPP1 mutations cause both generalized arterial calcification of infancy and autosomal-recessive hypophosphatemic rickets. *American journal of human genetics* **86**, 267-272.

Lories, R. J. and Luyten, F. P. (2011). The bone-cartilage unit in osteoarthritis. *Nature reviews. Rheumatology* **7**, 43-49.

Mak, K. K., Bi, Y., Wan, C., Chuang, P. T., Clemens, T., Young, M. and Yang, Y. (2008a). Hedgehog signaling in mature osteoblasts regulates bone formation and resorption by controlling PTHrP and RANKL expression. *Dev Cell* **14**, 674-688.

Mak, K. K., Chen, M. H., Day, T. F., Chuang, P. T. and Yang, Y. (2006). Wnt/beta-catenin signaling interacts differentially with Ihh signaling in controlling endochondral bone and synovial joint formation. *Development* **133**, 3695-3707.

Mak, K. K., Kronenberg, H. M., Chuang, P. T., Mackem, S. and Yang, Y. (2008b). Indian hedgehog signals independently of PTHrP to promote chondrocyte hypertrophy. *Development* **135**, 1947-1956.

McLeod, M. J. (1980). Differential staining of cartilage and bone in whole mouse fetuses by alcian blue and alizarin red S. *Teratology* **22**, 299-301.

Murshed, M., Harmey, D., Millan, J. L., McKee, M. D. and Karsenty, G. (2005). Unique coexpression in osteoblasts of broadly expressed genes accounts for the spatial restriction of ECM mineralization to bone. *Genes & development* **19**, 1093-1104.

Nakashima, K., Zhou, X., Kunkel, G., Zhang, Z., Deng, J. M., Behringer, R. R. and de Crombrugghe, B. (2002). The novel zinc finger-containing transcription factor osterix is required for osteoblast differentiation and bone formation. *Cell* **108**, 17-29.

Neuhold, L. A., Killar, L., Zhao, W., Sung, M. L., Warner, L., Kulik, J., Turner, J., Wu, W., Billinghurst, C., Meijers, T., et al. (2001). Postnatal expression in hyaline cartilage of constitutively active human collagenase-3 (MMP-13) induces osteoarthritis in mice. *The Journal of clinical investigation* **107**, 35-44.

Nitschke, Y., Baujat, G., Botschen, U., Wittkampf, T., du Moulin, M., Stella, J., Le Merrer, M., Guest, G., Lambot, K., Tazarourte-Pinturier, M. F., et al. (2012). Generalized arterial calcification of infancy and pseudoxanthoma elasticum can be caused by mutations in either ENPP1 or ABCC6. *American journal of human genetics* **90**, 25-39.

Nitschke, Y. and Rutsch, F. (2012). Generalized arterial calcification of infancy and pseudoxanthoma elasticum: two sides of the same coin. *Frontiers in genetics* **3**, 302.

North, R. A. (2002). Molecular physiology of P2X receptors. *Physiological reviews* **82**, 1013-1067.

Okawa, A., Ikegawa, S., Nakamura, I., Goto, S., Moriya, H. and Nakamura, Y. (1998). Mapping of a gene responsible for twy (tip-toe walking Yoshimura), a mouse model of ossification of the posterior longitudinal ligament of the spine (OPLL). *Mammalian genome : official journal of the International Mammalian Genome Society* **9**, 155-156.

Park, J., Gebhardt, M., Golovchenko, S., Perez-Branguli, F., Hattori, T., Hartmann, C., Zhou, X., deCrombrugghe, B., Stock, M., Schneider, H., et al. (2015). Dual pathways to endochondral osteoblasts: a novel chondrocyte-derived osteoprogenitor cell identified in hypertrophic cartilage. *Biology open* **4**, 608-621.

Regard, J. B., Cherman, N., Palmer, D., Kuznetsov, S. A., Celi, F. S., Guettier, J. M., Chen, M., Bhattacharyya, N., Wess, J., Coughlin, S. R., et al. (2011). Wnt/beta-catenin signaling

is differentially regulated by Galpha proteins and contributes to fibrous dysplasia. *Proc Natl Acad Sci U S A* **108**, 20101-20106.

Regard, J. B., Malhotra, D., Gvozdenovic-Jeremic, J., Josey, M., Chen, M., Weinstein, L. S., Lu, J., Shore, E. M., Kaplan, F. S. and Yang, Y. (2013). Activation of Hedgehog signaling by loss of GNAS causes heterotopic ossification. *Nat Med* **19**, 1505-1512.

Rodda, S. J. and McMahon, A. P. (2006). Distinct roles for Hedgehog and canonical Wnt signaling in specification, differentiation and maintenance of osteoblast progenitors. *Development* **133**, 3231-3244.

Ruf, N., Uhlenberg, B., Terkeltaub, R., Nurnberg, P. and Rutsch, F. (2005). The mutational spectrum of ENPP1 as arising after the analysis of 23 unrelated patients with generalized arterial calcification of infancy (GACI). *Human mutation* **25**, 98.

Rutsch, F., Ruf, N., Vaingankar, S., Toliat, M. R., Suk, A., Hohne, W., Schauer, G., Lehmann, M., Roscioli, T., Schnabel, D., et al. (2003). Mutations in ENPP1 are associated with 'idiopathic' infantile arterial calcification. *Nat Genet* **34**, 379-381.

Rutsch, F., Vaingankar, S., Johnson, K., Goldfine, I., Maddux, B., Schauerte, P., Kalhoff, H., Sano, K., Boisvert, W. A., Superti-Furga, A., et al. (2001). PC-1 nucleoside triphosphate pyrophosphohydrolase deficiency in idiopathic infantile arterial calcification. *The American journal of pathology* **158**, 543-554.

Sellam, J. and Berenbaum, F. (2010). The role of synovitis in pathophysiology and clinical symptoms of osteoarthritis. *Nature reviews. Rheumatology* **6**, 625-635.

Serrano, R. L., Yu, W. and Terkeltaub, R. (2014). Mono-allelic and bi-allelic ENPP1 deficiency promote post-injury neointimal hyperplasia associated with increased C/EBP homologous protein expression. *Atherosclerosis* **233**, 493-502.

Spector, T. D. and MacGregor, A. J. (2004). Risk factors for osteoarthritis: genetics. *Osteoarthritis and cartilage* **12 Suppl A**, S39-44.

St-Jacques, B., Hammerschmidt, M. and McMahon, A. P. (1999). Indian hedgehog signaling regulates proliferation and differentiation of chondrocytes and is essential for bone formation. *Genes Dev* **13**, 2072-2086.

Stefan, C., Jansen, S. and Bollen, M. (2005). NPP-type ectophosphodiesterases: unity in diversity. *Trends in biochemical sciences* **30**, 542-550.

Stone, D. M., Hynes, M., Armanini, M., Swanson, T. A., Gu, Q., Johnson, R. L., Scott, M. P., Pennica, D., Goddard, A., Phillips, H., et al. (1996). The tumour-suppressor gene patched encodes a candidate receptor for Sonic hedgehog. *Nature* **384**, 129-134.

Tchetina, E. V. (2011). Developmental mechanisms in articular cartilage degradation in osteoarthritis. *Arthritis* **2011**, 683970.

Topol, L., Jiang, X., Choi, H., Garrett-Beal, L., Carolan, P. J. and Yang, Y. (2003). Wnt-5a inhibits the canonical Wnt pathway by promoting GSK-3-independent beta-catenin degradation. *The Journal of cell biology* **162**, 899-908.

Valdes, A. M., Doherty, M. and Spector, T. D. (2008). The additive effect of individual genes in predicting risk of knee osteoarthritis. *Annals of the rheumatic diseases* **67**, 124-127.

Vortkamp, A., Lee, K., Lanske, B., Segre, G. V., Kronenberg, H. M. and Tabin, C. J. (1996). Regulation of rate of cartilage differentiation by Indian hedgehog and PTH-related protein. *Science* **273**, 613-622.

Wang, F., Flanagan, J., Su, N., Wang, L. C., Bui, S., Nielson, A., Wu, X., Vo, H. T., Ma, X. J. and Luo, Y. (2012). RNAscope: a novel in situ RNA analysis platform for formalin-fixed, paraffin-embedded tissues. *The Journal of molecular diagnostics : JMD* **14**, 22-29.

Yang, G., Zhu, L., Hou, N., Lan, Y., Wu, X. M., Zhou, B., Teng, Y. and Yang, X. (2014a). Osteogenic fate of hypertrophic chondrocytes. *Cell research* **24**, 1266-1269.

Yang, L., Tsang, K. Y., Tang, H. C., Chan, D. and Cheah, K. S. (2014b). Hypertrophic chondrocytes can become osteoblasts and osteocytes in endochondral bone formation. *Proceedings of the National Academy of Sciences of the United States of America* **111**, 12097-12102.

Zhang, J., Dyment, N. A., Rowe, D. W., Siu, S. Y., Sundberg, J. P., Uitto, J. and Li, Q. (2016). Ectopic mineralization of cartilage and collagen-rich tendons and ligaments in Enpp1asj-2J mice. *Oncotarget* **7**, 12000-12009.

Zhou, X., von der Mark, K., Henry, S., Norton, W., Adams, H. and de Crombrugghe, B. (2014). Chondrocytes transdifferentiate into osteoblasts in endochondral bone during development, postnatal growth and fracture healing in mice. *PLoS genetics* **10**, e1004820.

Figures

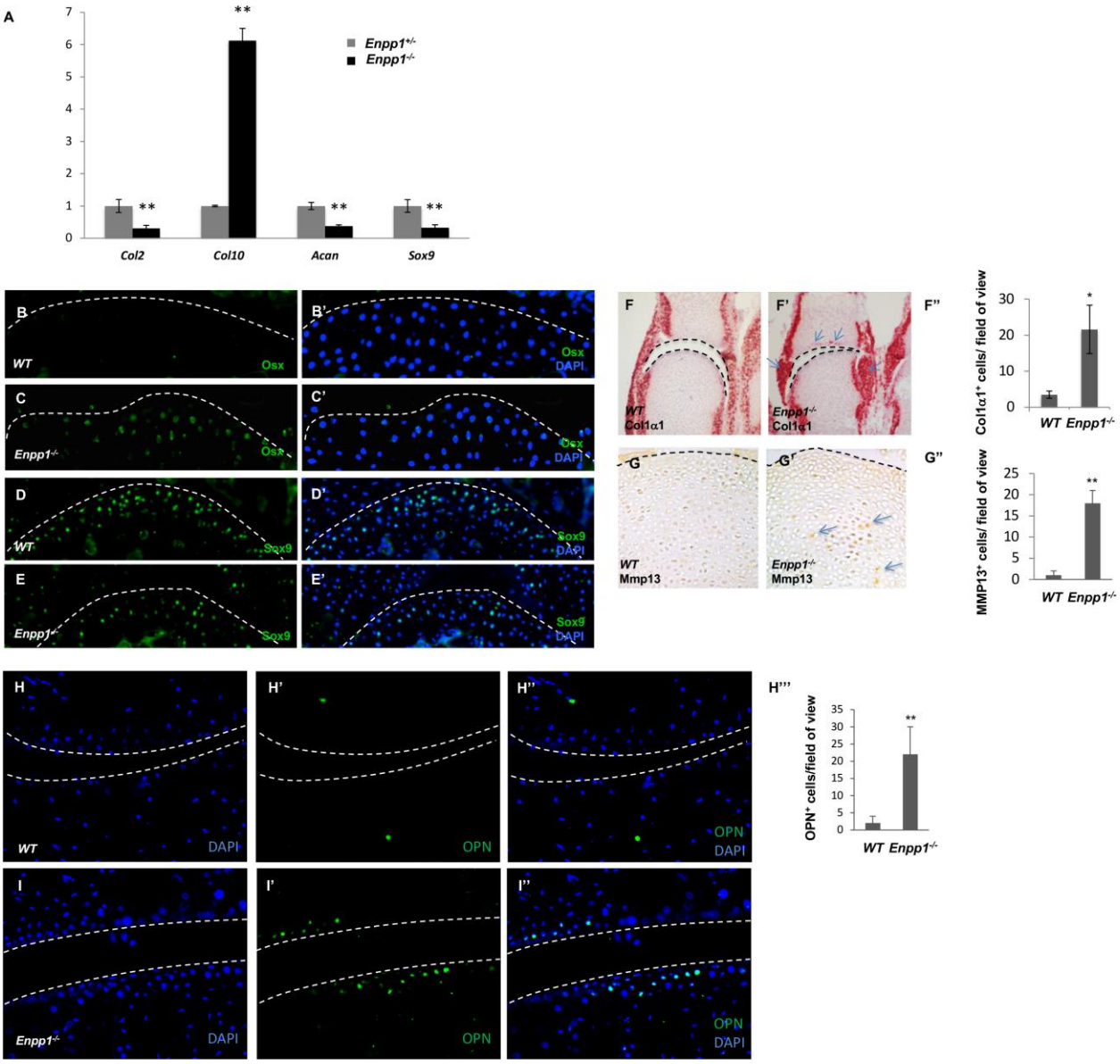

Fig. 1. Ectopic expression of hypertrophic chondrocyte and osteoblast markers in the *Enpp1*$^{-/-}$ metacarpophalangeal joint

(A) qRT-PCR analysis of cartilage specific markers and hypertrophic markers expressed in the metacarpophalangeal joints of *Enpp1*$^{-/-}$ and wild type (WT) control

mice at 1 month of age (SD; n=3) *P < 0.05, **P < 0.01 by student-t test. (B-E') Phalangeal joint sections from 1 month old WT and *Enpp1*$^{-/-}$ mice were stained with antibodies against Osx (B-C') and Sox9 (D-E'). Nucleus were shown by DAPI staining. (F-F") *Col1a1* mRNA expression detected by *in situ* hybridization with the RNAscope technology in the metacarpophalangeal joint surface of new born pups *(*P2). The arrows indicate ectopic expression of *Col1a1* in the *Enpp1*$^{-/-}$ joint cartilage and capsule. The *Col1a1* expressing cells in the articular cartilage of the metacarpophalangeal joints were quantified as the number of Col1a1^{+}/ field of view under 40x objective magnification (n=4), *P < 0.05. (G- G'') Mmp13 expression in the joints of 1 month old WT and *Enpp1*$^{-/-}$ mice. MMP13^{+} cells were quantified as the number of MMP13^{+} cells/ field of view (G''). (H- I'') Opn expression in the joints of 1 month old WT and *Enpp1*$^{-/-}$ mice. Opn^{+} positive cells were quantified as the number of Opn^{+} cells/ field of view (500x400μm) (H'''). **P < 0.01 by student-t test. Dotted lines indicated the surface of articular cartilage.

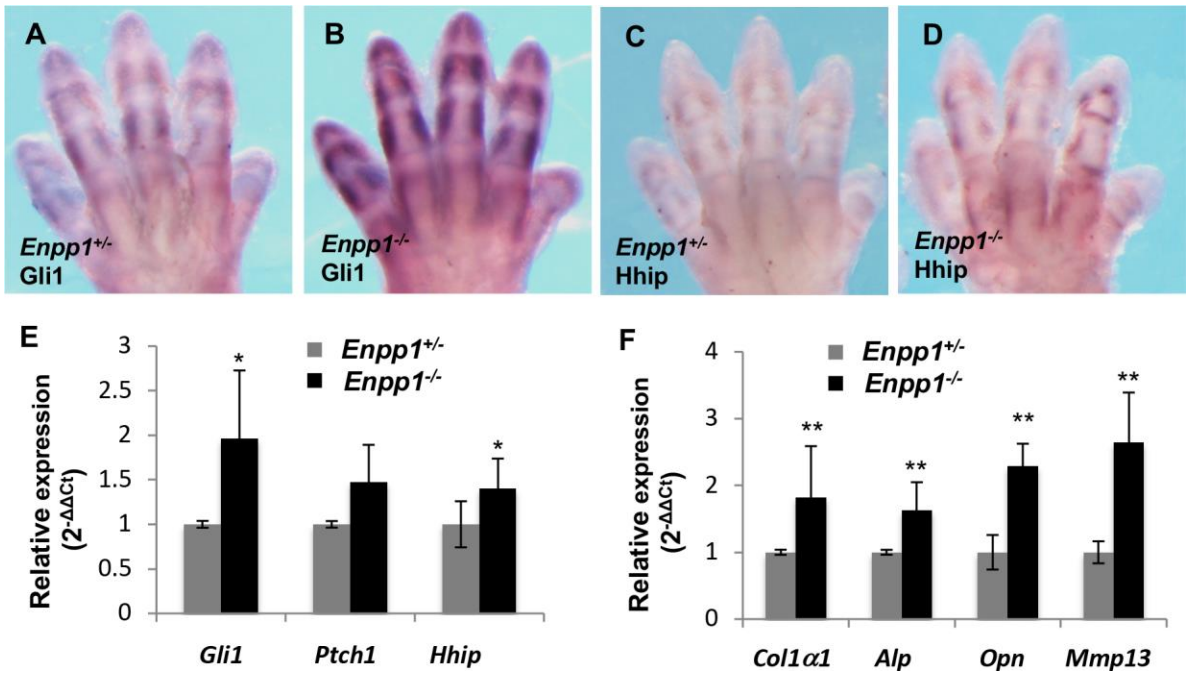

Fig. 2. Increased Hh signaling activity in the *Enpp1*$^{-/-}$ embryo

(A-D) Expression of Hh signaling targets *Gli1*, *Hhip* in E15.5 wild type and *Enpp1*$^{-/-}$ forelimbs shown by whole mount *in situ* hybridization. *Gli1, Hhip* mRNA levels were up-regulated in the limbs of the *Enpp1*$^{-/-}$ embryos. (E-F) qRT-PCR analysis of Hh target gene expression in the forelimbs of E15.5 embryos (n=3) *P < 0.05, **P < 0.01 by student-t test.

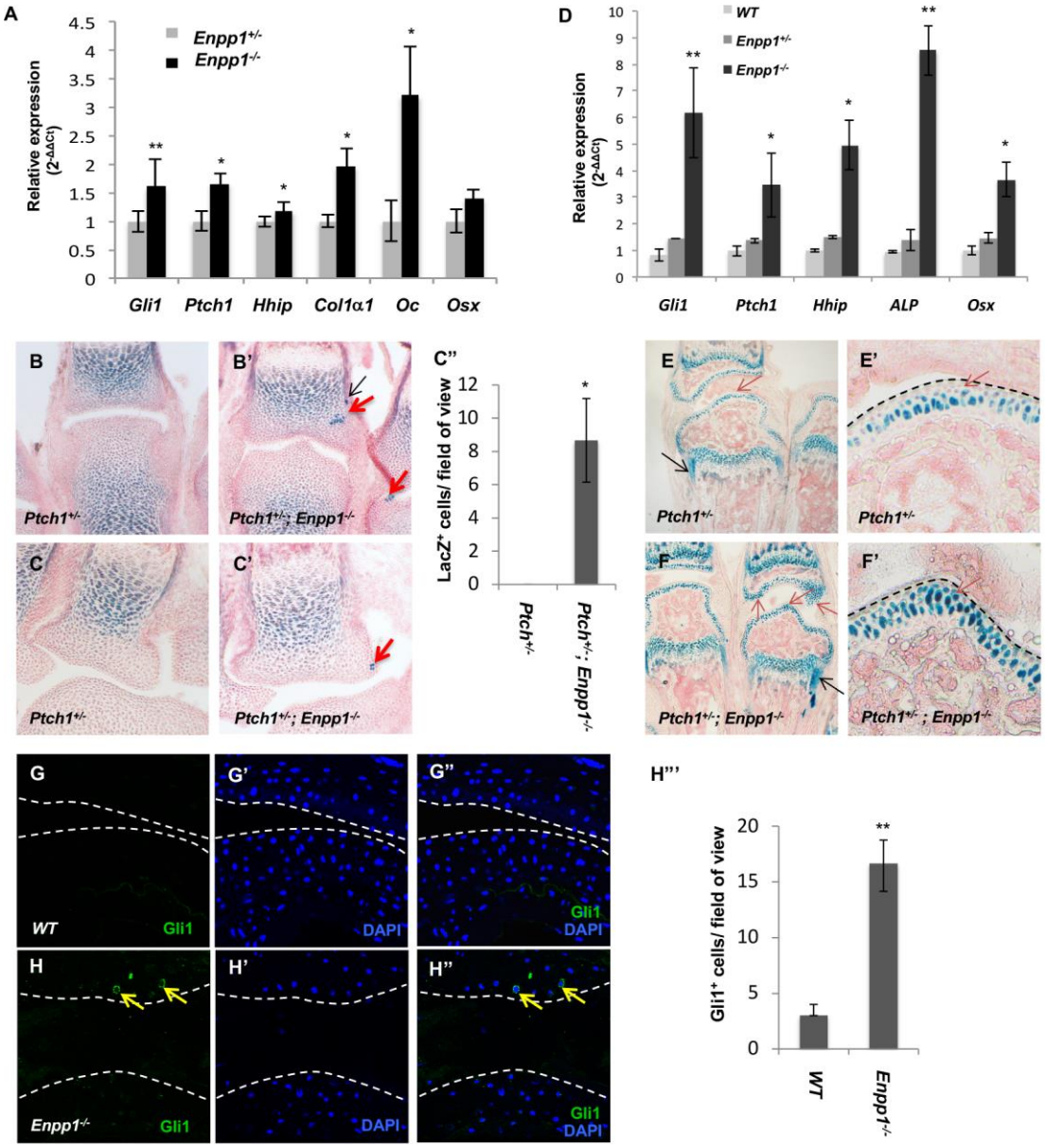

Fig. 3. Increased Hh signaling activity in postnatal *Enpp1*$^{-/-}$ mutant mice

(A) qRT-PCR analysis of gene expression of Hh targets and osteoblast markers in the front paws of the postnatal day 2 (P2) mice (n=3) *P < 0.05, **P < 0.01 by student-t test.. (B-C") LacZ staining of the metacarpophalangeal (B, B') and carpo-metacarpal joints (C, C') of P2 *Enpp1*$^{-/-}$ and *Enpp1*$^{-/-}$*; Ptch1*$^{+/-}$ mice. Ectopic *Ptch1-LacZ* expression was indicated by red arrows (articular cartilage) and black arrows (perichondrium). The

number of LacZ positive cells in the articular cartilage of the metacarpophalangeal joints were quantified as the number of $LacZ^{+}$/ field of view under 40x objective magnification (n=3), *P < 0.05. (D) qRT-PCR analysis of Hh target and osteogenic genes expressed in the front paws of the one month old *Enpp1*$^{-/-}$ mice (n=3) *P < 0.05, **P < 0.01 by student-t test. (E-F') Hh signaling activity was detected by *LacZ* expression in the metacarpophalangeal joints from the 3 weeks old *Ptch1*$^{+/-}$, and *Ptch1*$^{+/-}$*; Enpp1*$^{-/-}$ mice. Black arrows show Hh activity in the perichondrium of metacarpal bone. The articular cartilage is shown in higher magnification (E', F'). Red arrows indicate the LacZ positive chondrocytes. (G-H"') Phalangeal joint sections from 2 months old wild type and *Enpp1*$^{-/-}$ mice were stained with antibodies against Gli1. Nucleus were shown by DAPI staining. Gli1 expression was detected in the articular chondrocyte of *Enpp1*$^{-/-}$, but not wild type mice. The number of Gli1 positive cells in the articular cartilage were quantified as the number of $Gli1^{+}$/ field of view under 40x objective magnification (n=3). *P < 0.05, **P < 0.01 by student t test. Dotted lines indicated the surface of articular cartilage.

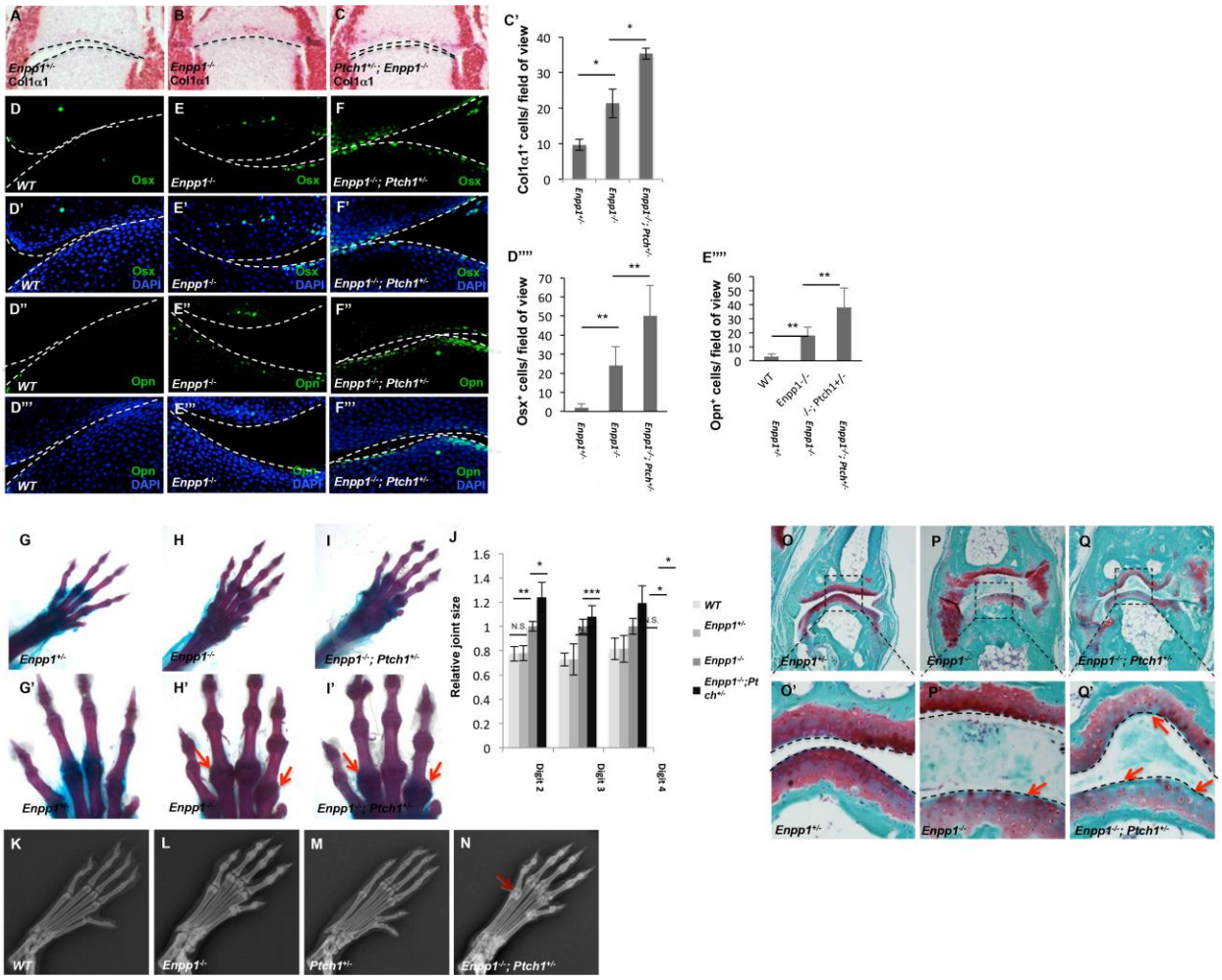

Fig.4. Enhanced joint calcification by enhancing Hh signaling in the *Enpp1*$^{-/-}$ mice

(A-C) *Col1a1* expression was detected by *in situ* hybridization of the phalangeal joint sections from P2 mice. (C') The number of Col1a1 positive cells in the articular cartilage of the metacarpophalangeal joints were quantified as the number of Col1a1^{+}/ field of view under 40x objective magnification (n=3), *P < 0.05. (D-F"') Fluorescent immunostaining of Osx and Opn in the phalangeal joint sections of *WT, Enpp1*$^{-/-}$ and *Enpp1*$^{-/-}$*; Ptch1*$^{+/-}$ mice, which were P2 littermates. Osx^{+} and Opn^{+} cells were quantified as the number of Osx^{+}/ field of view (500x300μm) (D'''') and Opn^{+}/ field of view

(500x300μm) (E’’’). **P < 0.01 by student-t test. (G-I’) Representative images of Alcian blue and Alizarin red stained forelimbs from 3 months old *Enpp1*$^{+/-}$ (G), *Enpp1*$^{-/-}$ (H), and *Enpp1*$^{-/-}$*; Ptch1*$^{+/-}$ (I) mice. (G’, H’, I’) Phalangeal joints are shown in higher magnification. Arrows indicated the enlarged metacarpophalangeal joints. (J) Quantification of the sizes of the metacarpophalangeal joints in *WT*, *Enpp1*$^{+/-}$, *Enpp1*$^{-/-}$*; Ptch1*$^{+/-}$ and *Enpp1*$^{-/-}$ mice. Littermates of *Enpp1*$^{-/-}$*; Ptch1*$^{+/-}$ and *Enpp1*$^{-/-}$ were used in this experiment (n=3), NS, not significant. *P < 0.05, **P < 0.01 by student t test. (K-N) Representative X-ray images of the hindlimbs from 4 months old mice. Arrow indicates enhanced calcification in the phalangeal joint of *Enpp1*$^{-/-}$*; Ptch1*$^{+/-}$ mice. (O-Q’) Safranin-O staining of sections of the metacarpophalangeal joints from forelimbs of 3 months old *Enpp1*$^{+/-}$ (O, O’), *Enpp1*$^{-/-}$ (P, P’), *Enpp1*$^{-/-}$*; Ptch1*$^{+/-}$ (Q, Q’) mice. Arrows indicate reduced Safranin-O staining. Dotted lines indicated the surface of articular cartilage.

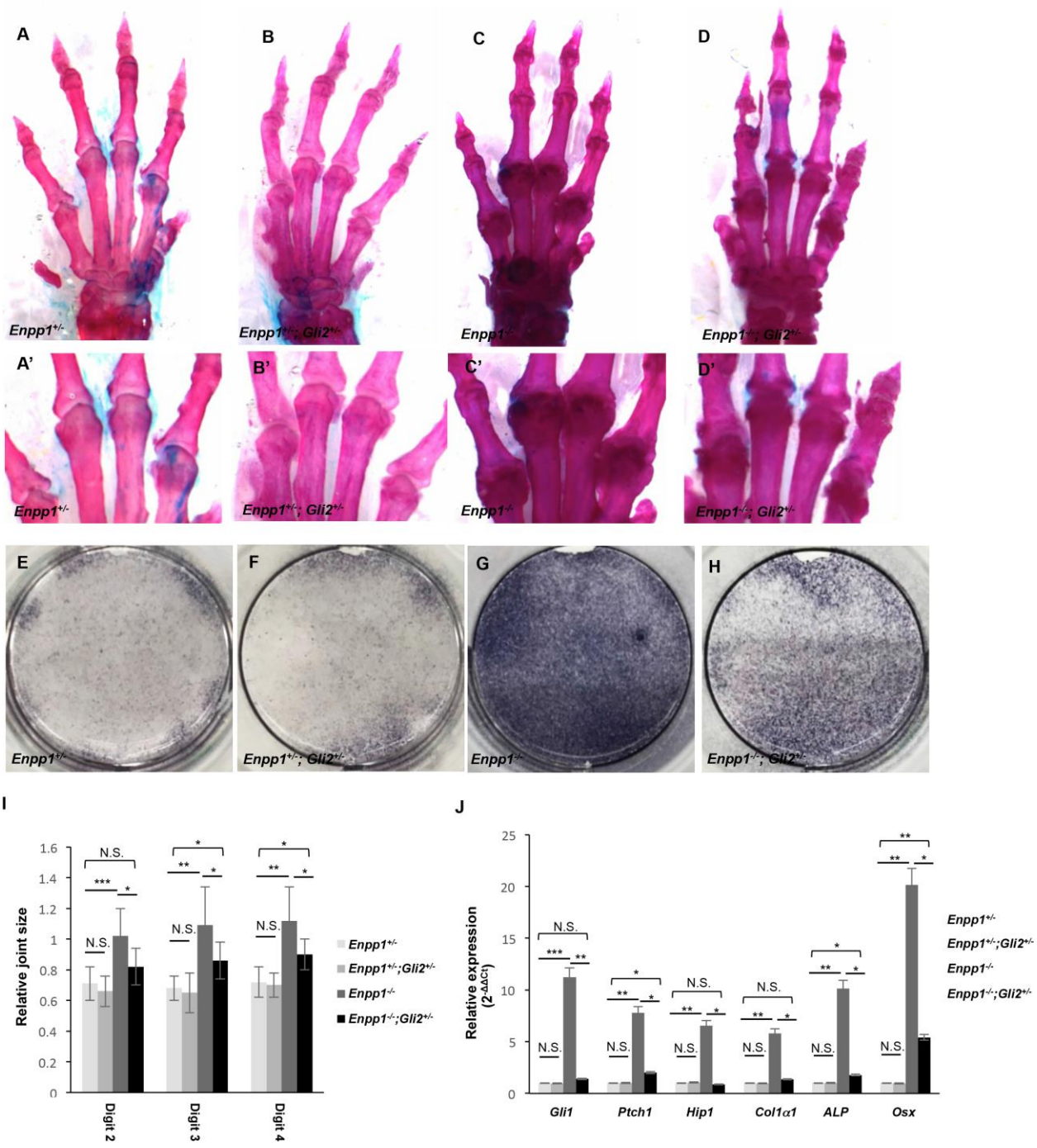

Fig. 5. Reduced Hh signaling activity partially rescued joint calcification of *Enpp1*$^{-/-}$ mice

(A-D) Representative images of Alcian blue and Alizarin red stained forelimbs from 3 months old *Enpp1*$^{-/-}$ (A), *Enpp1*$^{+/-}$; *Gli2*$^{+/-}$ (B), *Enpp1*$^{-/-}$ (C), *Enpp1*$^{-/-}$; *Gli2*$^{+/-}$ (D) mice. (A', B', C', D') Phalangeal joints were shown with higher magnification. (E-G) Representative Alkaline phosphatase staining of SMPs from wild type (E), *Enpp1*$^{+/-}$; *Gli2*$^{+/-}$ (F), *Enpp1*$^{-/-}$ (G), and *Enpp1*$^{-/-}$; *Gli2*$^{+/-}$ mice (H) cultured in osteogenic medium for 7 days. (I) Quantification of the relative metacarpophalangeal joint sizes. Littermates were used in this experiment, n=4. (J) qRT-PCR analysis of Hh target and osteoblast genes expressed in SMPs of indicated genotypes. SMPs were cultured in osteogenic medium for 7 days (n=3). *P < 0.05, **P < 0.01, ***P < 0.001 by student t test.

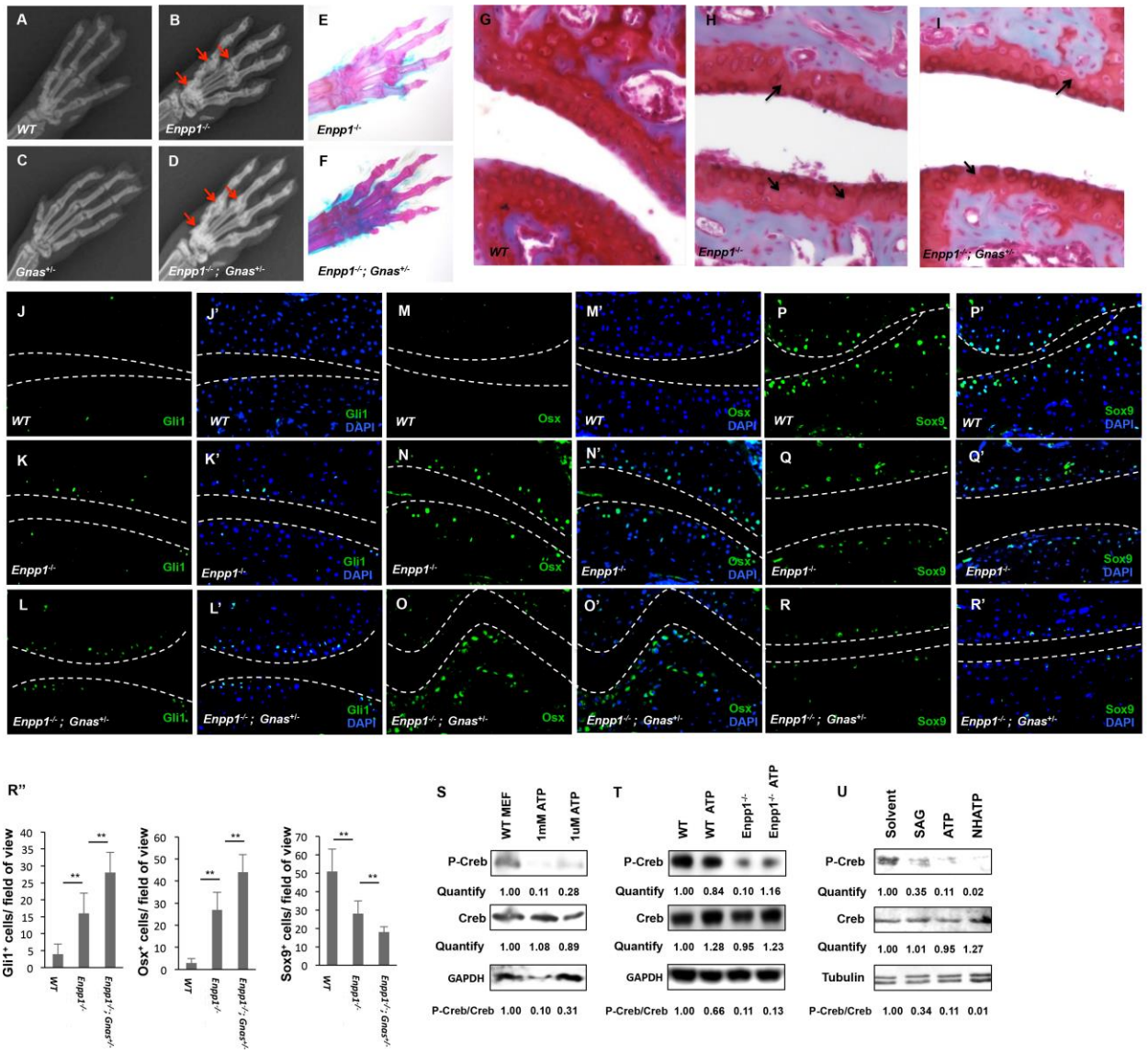

Fig. 6. Ectopic joint calcification in *Enpp1*$^{-/-}$ mutants was enhanced by reduced *Gnas*

(A-D) Representative X-ray images of the forelimbs of the 2 months old wild type, *Enpp1*$^{-/-}$, *Gnas*$^{+/-}$, and *Enpp1*$^{-/-}$*; Gnas*$^{+/-}$ mice. *Gnas*$^{+/-}$ enhanced the joint calcification of the *Enpp1*$^{-/-}$ mice. This data indicated that Enpp1 may signal through Gα_s in regulating

cartilage calcification. (E-F) Representative Alizarin Red and Alcian blue staining of forelimbs from the *Enpp1*$^{-/-}$ and the *Enpp1*$^{-/-}$*; Gnas*$^{+/-}$ mice at 2.5 months of age. More ectopic mineralization can be found around the joints of the *Enpp1*$^{-/-}$*; Gnas*$^{+/-}$ mice compared with the *Enpp1*$^{-/-}$ mice. (G-I) Representative Safranin-O staining of phalangeal joint sections from forelimbs of 1 month old mice. Arrows indicate reduced Safranin-O staining and reduced cartilage thickness. (J-R'') Sections of phalangeal joints from 1 months old WT, *Enpp1*$^{-/-}$, *Enpp1*$^{-/-}$*; Gnas*$^{+/-}$ mice were stained with antibodies against Gli1 (J-L'), Osx (M-O') and Sox9 (P-R'). Gli1, Osx and Sox9 positive cells were counted and quantified as the number of Gli1^{+}/ field of view, Osx^{+}/ field of view and Sox9^{+}/ field of view (500x400μm) (R''). **P < 0.01 by student t test. Nucleus were shown by DAPI staining. White lines indicated the surface of articular cartilage. (S) PKA activity measured by p-Creb levels in MEF cells from the wild type mice. Cells were treated for 5 min with ATP of indicated concentration. (T) Chondrocytes isolated from P0 WT and *Enpp1*$^{-/-}$ mice were treated with 1mM ATP for 5 min. P-Creb and total Creb protein levels were detected by Western blotting. (U) WT MEF cells were treated with 100nM SAG, 0.1mM ATP, or 0.1mM NHATP for 10 min (U). p-Creb, total Creb and Tubulin protein levels were detected by Western blotting. Protein bands in the Western blotting were quantified by densitometry and analyzed using Image J. The numbers indicate relative gray scale values of P-Creb and Creb in each lane and P-Creb/Creb ratio was calculated.

Supplementary Figure. 1

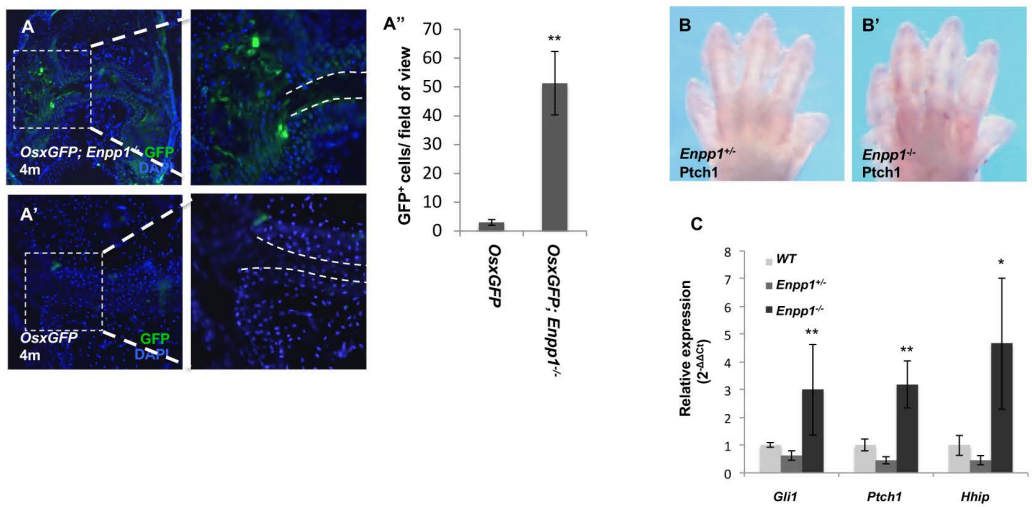

Supplementary Fig. 1. Increased Hh signaling activity in the joints of *Enpp1*$^{-/-}$ mice
(A-A") Direct fluorescence of OsxGFP with DAPI staining on the phalangeal joint sections from 4 months old *OsxGFPcre; Enpp1*$^{-/-}$ mice (A) or *OsxGFPCre* mice (A'). The number of GFP positive cells in the articular cartilage of the metacarpophalangeal joints were quantified as the number of GFP^{+}/ field of view under 40x objective magnification (n=4), *P < 0.05 (A"). (B-B') The E12.5 *Enpp1*$^{+/-}$ and *Enpp1*$^{-/-}$ embryos were collected for whole mount *in situ* hybridization with the Ptch1 riboprobe. (C) qRT-PCR analysis of Hh target genes and osteoblast genes expressed in the front paws of the 3 months old mice (n=3). *P < 0.05, **P < 0.01, ***P < 0.001 by student t test.

Supplementary Figure. 2

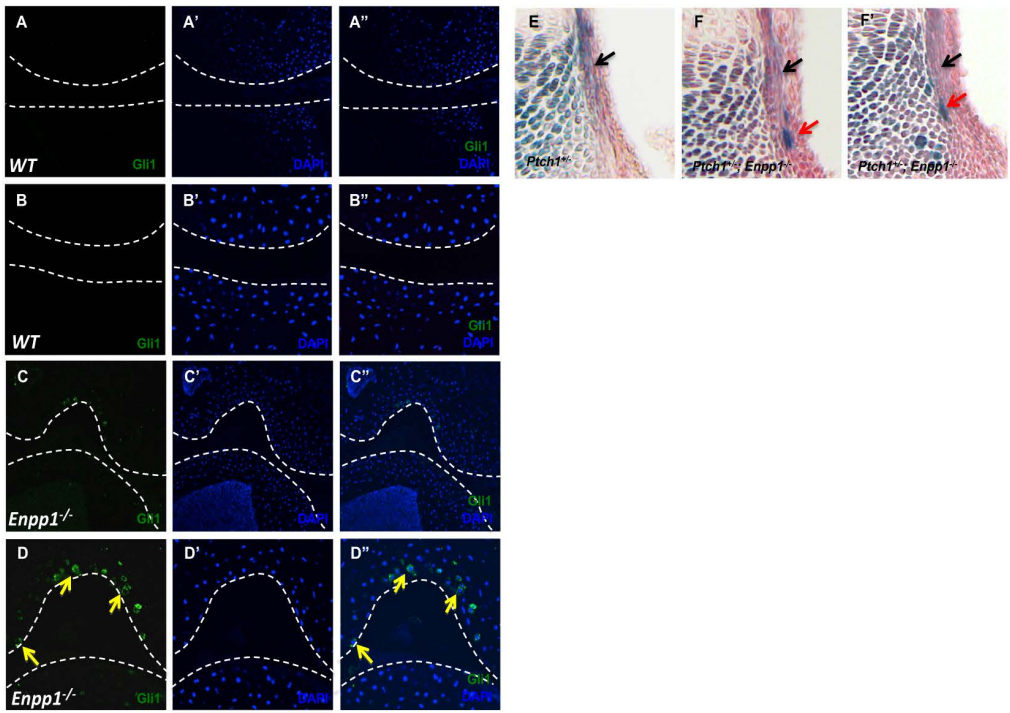

Supplementary Fig. 2. Ectopic expression of Gli1 in the articular cartilage of *Enpp1*$^{-/-}$ at 4 months of age
(A-D") Immunofluorescent Gli1 staining of phalangeal joint sections from 4 months old mice. Nucleus were shown by DAPI staining. (B-B", D-D") Enlarged images of (A-A") and (C-C") respectively. Gli1 expression was detected in the articular chondrocyte of *Enpp1*$^{-/-}$ mice (Yellow arrows), not in the wild type ones. (E-F') Hh signaling activity was detected by *Ptch1-LacZ* expression in the metacarpophalangeal joints from the P2 *Ptch1*$^{+/-}$, and *Ptch1*$^{+/-}$*; Enpp1*$^{-/-}$ mice. *Ptch1-LacZ* expression in the perichondrium is shown by back arrows and aberrant ectopic upregulation of *Ptch1-LacZ* is shown by red arrows.

Supplementary Figure. 3

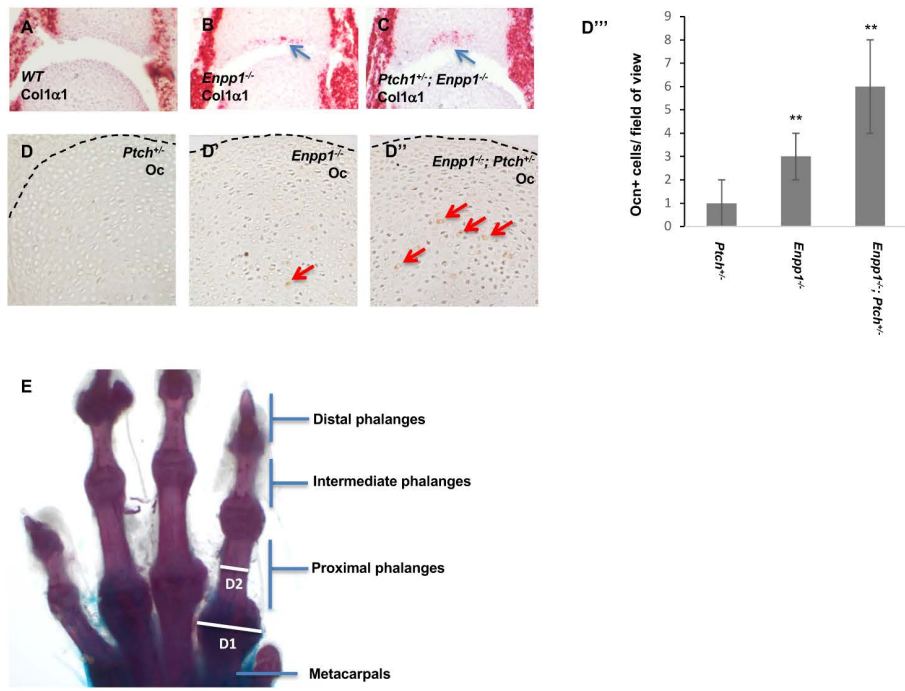

Supplementary Fig. 3. Enhanced osteoblastic differentiation in the *Ptch1*$^{+/-}$*; Enpp1*$^{-/-}$ joint and the measurement of forelimb phalangeal joint size

(A-C) Col1a1 expression in the phalangeal joint section of P2 mice was detected by *in situ* hybridization. (D-D''') Analysis of Oc expression in the articular cartilage (n=3). Oc positive cells number were counted and quantified under 40X magnification / field (D'''). **P < 0.01 by student t test. Forelimbs were used for quantification of the metacarpophalangeal joint size. The joint sizes were measured by image J. The metacarpophalangeal joint size (D1) and the diameters of the proximal phalanges (D2) were measured, then the ratios of D1/D2 of each digit were calculated as the relative joint size and used for the statistical analysis (E).

Supplementary Figure. 4

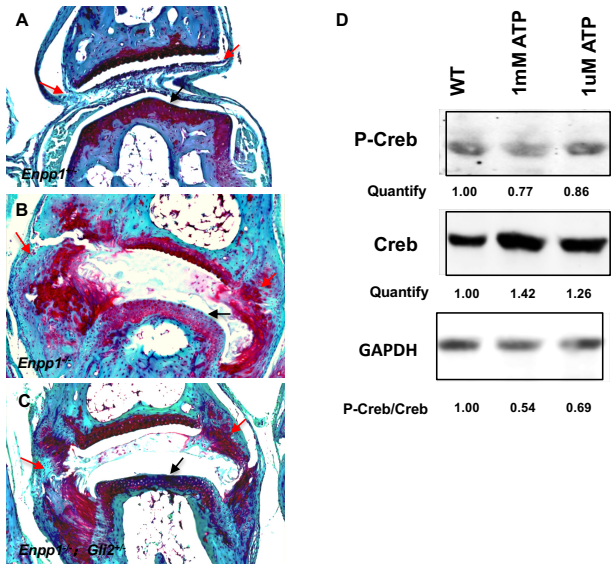

Supplementary Fig. 4. Reduced join phenotypes in the *Gli2*$^{+/-}$*; Enpp1*$^{-/-}$ mice and p-Creb regulation by ATP in synovial cells

(A-C) Safranin-O staining of metacarpophalangeal joint sections from forelimbs of 10 weeks old mice. Black arrows indicate articular cartilage and red arrows indicate joint capsule. (D) PKA activity measured by p-Creb/ Creb ratio in primary synovial cells from the wild type mice. Cells were treated for 10 min with indicated ATP concentrations. Protein bands in the Western blotting were quantified by densitometry and analyzed using Image J. The numbers indicate relative gray scale values of P-Creb and Creb in each lane and P-Creb/Creb ratio was calculated.

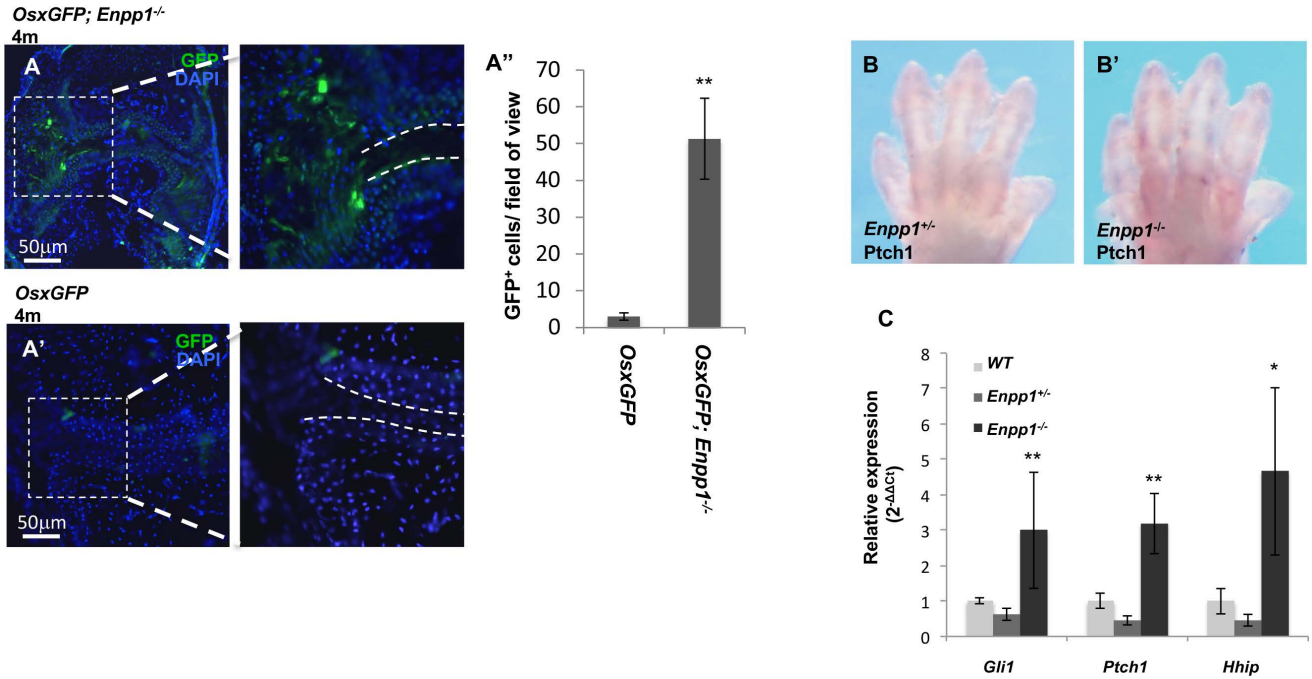

Supplementary Fig. 1. Increased Hh signaling activity in the joints of *Enpp1*$^{-/-}$ mice
(A-A") Direct fluorescence of OsxGFP with DAPI staining on the phalangeal joint sections from 4 months old *OsxGFPcre; Enpp1*$^{-/-}$ mice (A) or *OsxGFPCre* mice (A'). The number of GFP positive cells in the articular cartilage of the metacarpophalangeal joints was quantified as the number of GFP^{+}/ field of view under 40x objective magnification (n=4) (A").
(B-B') The E12.5 *Enpp1*$^{+/-}$ and *Enpp1*$^{-/-}$ embryos were collected for whole mount *in situ* hybridization with the Ptch1 riboprobe. (C) qRT-PCR analysis of Hh target genes and osteoblast genes expressed in the front paws of the 3 months old mice (n=3). *P < 0.05, **P < 0.01, ***P < 0.001 by student t test.

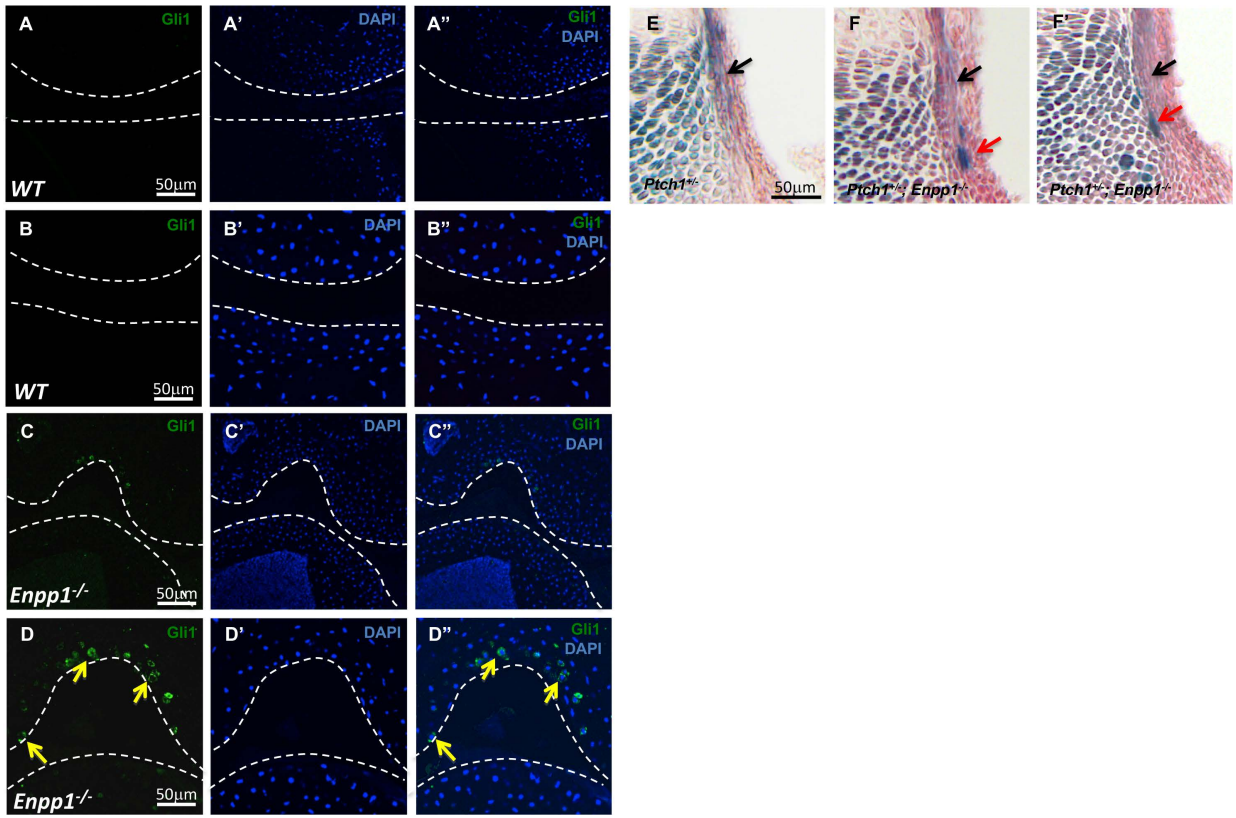

Supplementary Fig. 2. Ectopic expression of Gli1 in the articular cartilage of *Enpp1*$^{-/-}$ at 4 months of age
(A-D") Immunofluorescent Gli1 staining of phalangeal joint sections from 4 months old mice. Nucleus were shown by DAPI staining. (B-B", D-D") Enlarged images of (A-A") and (C-C") respectively. Gli1 expression was detected in the articular chondrocyte of *Enpp1*$^{-/-}$ mice (Yellow arrows), not in the wild type ones. (E-F') Hh signaling activity was detected by *Ptch1-LacZ* expression in the metacarpophalangeal joints from the P2 *Ptch1*$^{+/-}$, and *Ptch1*$^{+/-}$*; Enpp1*$^{-/-}$ mice. *Ptch1-LacZ* expression in the perichondrium is shown by back arrows and aberrant ectopic upregulation of *Ptch1-LacZ* is shown by red arrows.

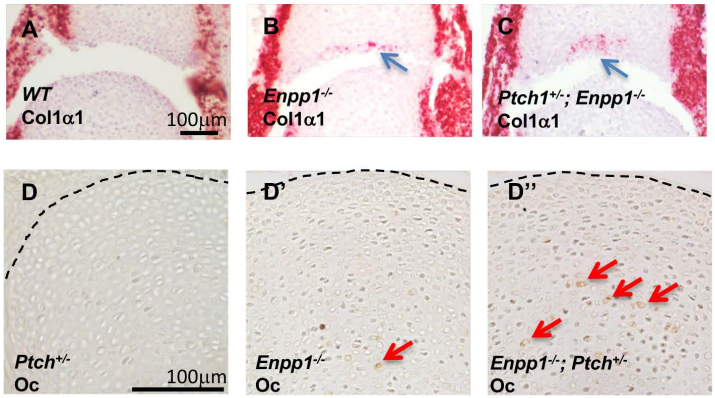

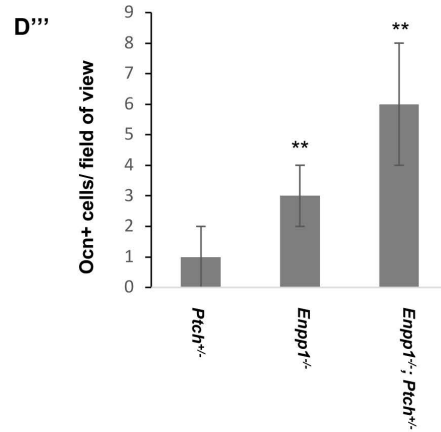

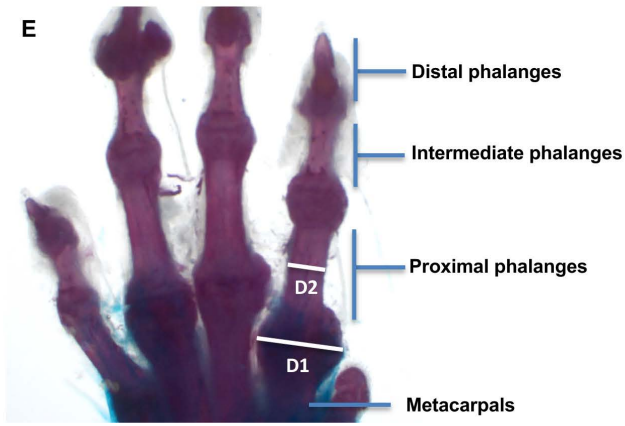

Supplementary Fig. 3. Enhanced osteoblastic differentiation in the *Ptch1*$^{+/-}$*; Enpp1*$^{-/-}$ joint and the measurement of forelimb phalangeal joint size

(A-C) Col1a1 expression in the phalangeal joint section of P2 mice was detected by *in situ* hybridization. (D-D''') Analysis of Oc expression in the articular cartilage (n=3). Oc positive cells number were counted and quantified under 40X magnification / field (D'''). **P < 0.01 by student t test. Forelimbs were used for quantification of the metacarpophalangeal joint size. The joint sizes were measured by image J. The metacarpophalangeal joint size (D1) and the diameters of the proximal phalanges (D2) were measured, then the ratios of D1/D2 of each digit were calculated as the relative joint size and used for the statistical analysis (E).

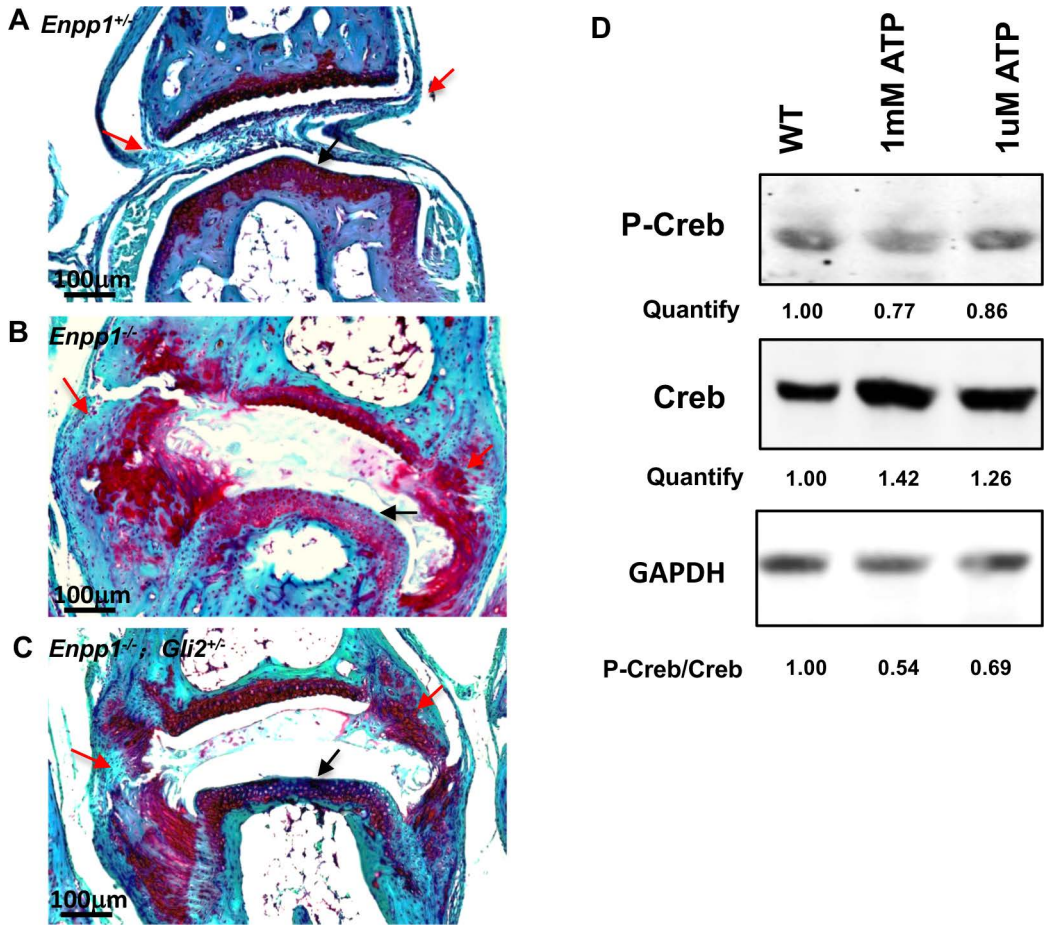

Supplementary Fig. 4. Reduced join phenotypes in the *Gli2*$^{+/-}$; *Enpp1*$^{-/-}$ mice and p-Creb regulation by ATP in synovial cells

(A-C) Safranin-O staining of metacarpophalangeal joint sections from forelimbs of 10 weeks old mice. Black arrows indicate articular cartilage and red arrows indicate joint capsule. (D) PKA activity measured by p-Creb/ Creb ratio in primary synovial cells from the wild type mice. Cells were treated for 10 min with indicated ATP concentrations. Protein bands in the Western blotting were quantified by densitometry and analyzed using Image J. The numbers indicate relative gray scale values of P-Creb and Creb in each lane and P-Creb/Creb ratio was calculated.